LOW DOSE RADIATION INTERACTIONS WITH THE TRANSFORMATION GROWTH FACTOR (TGF)-BETA PATHWAY

A Dissertation

by

AMY JESSE MASLOWSKI

Submitted to the Office of Graduate Studies of
Texas A&M University
in partial fulfillment of the requirements for the degree of

DOCTOR OF PHILOSOPHY

August 2007

Major Subject: Nuclear Engineering

LOW DOSE RADIATION INTERACTIONS WITH THE TRANSFORMATION GROWTH FACTOR (TGF)-BETA PATHWAY

A Dissertation

by

AMY JESSE MASLOWSKI

Submitted to the Office of Graduate Studies of
Texas A&M University
in partial fulfillment of the requirements for the degree of

DOCTOR OF PHILOSOPHY

Approved by:

Chair of Committee,	John R. Ford
Committee Members,	Leslie A. Braby
	John W. Poston, Sr.
	Joanne R. Lupton
Head of Department,	John W. Poston, Sr.

August 2007

Major Subject: Nuclear Engineering

ABSTRACT

Low Dose Radiation Interactions with the

Transformation Growth Factor (TGF)-beta Pathway. (August 2007)

Amy Jesse Maslowski, B.S., College of Charleston

Chair of Advisory Committee: Dr. John R. Ford

A major limiting factor for long-term, deep-space missions is the radiation dose to astronauts. Because the dose to the astronauts is a mixed field of low- and high-LET radiation, there is a need to understand the effects of both radiation types on whole tissue; however, there are limited published data on the effects of high-LET (linear-energy-transfer) radiation on tissue. Thus, we designed a perfusion chamber system for rat trachea in order to mimic *in vivo* respiratory tissue. We successfully maintained the perfused tracheal tissue *ex vivo* in a healthy and viable condition for up to three days. In addition, this project studied the effects of high-LET Fe particles on the overall transformation growth factor (TGF)-beta response after TGF-beta inactivation and compared the results to the TGF-beta response post x-ray irradiation. It was found that a TGF-beta response could be measured in the perfused tracheal tissue, for x-ray and Fe particle irradiations, despite the high autofluorescent background intrinsic to tissue. However, after comparing the TGF-beta response of x-ray irradiation to High-Z-High-energy (HZE) irradiation, there was not a significant difference in radiation types. The TGF-beta response in x-ray and HZE irradiated perfusion chambers was also measured over time post irradiation. It was found that for 6 hour and 8 hour post irradiation, the

TGF-beta response was higher for lower doses of radiation than for higher doses. This is in contrast to the 0 hour fixation which found the TGF-beta response to increase with increased dose. The inverse relationship found for 6 hour and 8 hour fixation times may indicate a threshold response for TGF-beta response; i.e., for low doses, a threshold of dose must be reached for an immediate TGF-beta response, otherwise the tissue responds more slowly to the irradiation damage. This result was unexpected and will require further investigation to determine if the threshold can be determined for the 250 kVp x-rays and 1 Gev Fe particles.

DEDICATION

To my mother and father;

Without whom I would never have made it to graduate school.

To my husband;

Without whom I would never have made it through graduate school.

ACKNOWLEDGMENTS

First, I would like to thank my committee for their guidance and advice in finishing my Ph.D. I would like to especially thank my advisor, Dr. Ford, for his unending patience. I could not have finished this with anyone less understanding. I would also like to thank those who pushed me through some of my low points in graduate school: Dr. Ryan, Dr. Charlton, and Dr. Bluhm.

I would like to acknowledge my Aggie family who kept me sane during this whole process: Jae, Lucile, Cable, Teresa, Civ, Repeat, Christian, Natela, David, Melissa, Casey, Katie, Toe Jam, Neicy, Angie, and Will. Thank you guys for not letting me take anything too seriously.

This research would not have been possible without the funding of the Office of Science (BER), U.S. Department of Energy, Grant No. DE-FG03-02ER63438 and the National Aeronautical and Space Administration Office of Biological and Physical Research (NASA/OBPR).

NOMENCLATURE

ECM	Extracellular Matrix
GCR	Galactic Cosmic Ray
HZE	High-Z-High-Energy
LAP	Latent Associated Peptide
LET	Linear Energy Transferred
LTBP	Latent TGF-beta Binding Protein
PCNA	Proliferating Cell Nuclear Antigen
SPE	Solar Particle Event
TGF-beta	Transformation Growth Factor-beta

TABLE OF CONTENTS

Page

LIST OF FIGURES

FIGURE Page

CHAPTER I

INTRODUCTION

Since space travel began, man has faced the challenges of leaving the earth's atmosphere to reach orbit and travel beyond. The environment a flight crew faces is drastically different than the terrestrial environment. On the earth's surface, biological processes are well adapted to the gravity of earth and are protected from the types and quantities of radiation found in space by earth's atmosphere and its intrinsic magnetic field. Microgravity and increased background radiation levels are known to cause specific risks for astronauts including muscle atrophy and calcium loss. Radiation risks will become serious problems for longer future missions that travel deeper into space. The future of space exploration depends on finding a solution to these challenges.

The most significant risk of deep and prolonged space travel identified thus far is calcium loss. Whole body calcium loss was found to reduce bone mineral density in the tibia, greater trochanter, femoral neck, and lumbar vertebrae by averages of 2.8%, 8.2%, 5.0%, and 6.2%, respectively, for seven astronauts who stayed on the Mir space station for four to six months. Skylab data showed the body loses 200 to 300 mg/d of calcium (*1*). Countermeasures are being tested in an effort to ameliorate the bone loss caused by extended flight times; however, nothing has been found to correct this loss.

This dissertation follows the style of *Radiation Research.*

More significantly, the reduction in bone density is indicative of a change in cellular processes and could have an effect on how the cell responds to DNA damage. Studies have addressed microgravity effects on a cell's response to ionizing radiation and have found no conclusive results. Early experiments found human leukocytes flown in space do have increased levels of chromosome deletions as compared to ground-level irradiations (*2*). However, these results could not be confirmed with subsequent experiments (*3*). Moreover, theoretical analysis of gravity's effects on DNA postulate that it should be negligible for structures smaller than the nucleus (*4*). Kiefer and Pross calculated that the gravitational energy would be orders of magnitude lower than the thermal energy of molecules due to gravity's dependence on mass. Current experiments have made only one thing clear: the biological responses to High-Z-High-Energy (HZE) particles in reduced gravity are not yet completely understood. Hence, focusing research on HZE biological effects for ground-level experiments may help correlate how microgravity changes the biological response to irradiations.

One of the most significant health risks of future space travel is exposure to the harsh radiation field beyond the protection of the earth's Van Allen belts. The crew on such missions will be exposed to a continuous spectrum of background galactic cosmic rays (GCR) in addition to intermittent energetic solar particle events (SPE). Both sources contribute to radiation risks to flight crews and each has unique properties and interactions with biological systems. The sources of GCR have yet to be positively identified, but are most probably supernova remnants accelerated by magnetic fields and

result in a generally isotropic field of high-energy charged particles. Of the charged particle spectrum, 98% are protons and heavy ions, and two percent are electrons and positrons ranging in energy from 10 MeV/n to 10 GeV/n (*5*). The particles that would contribute the most to the equivalent dose to astronauts in this spectrum are hydrogen, helium, carbon, neon, oxygen, silicon and iron. SPE are also a significant contributor to the dose to astronauts and usually occur at solar maximum; however there is no reliable method for predicting when and at what magnitude an SPE will occur. The SPE fluence can be greater than 10^{10} protons/cm^2 with energies greater than 10 MeV. In addition to large proton fluence, an SPE may consist of alpha particles and heavier nuclei; however, there is a shortage of data so risks due to SPE are difficult to determine. These two spectra are the major sources for equivalent dose to the crew during space flight, but since the spectra are not well known, their interactions in tissue and resulting estimation of equivalent doses are uncertain at present.

Radiation Effects

Ionizing radiation causes damage to cells and its DNA and can result in the formation of micronuclei and the induction of bystander effects. While much research has addressed these effects on biological systems, the effects of HZE particles are little studied and poorly understood. In order to better understand these effects, the interaction of HZE particles with cells and their effect is the present interest of this study.

The radiation environment in low earth orbit (LEO) consists of high energy protons, HZE particles and secondary radiation produced as a result of interactions with spaceship walls and tissue. Despite their low frequency, HZE particles are of great importance to risk because of their high ionization potential and their large contribution to equivalent dose. Unlike low-linear energy transfer (LET) radiation which has a tortuous path through tissue and spatially distributed energy deposition, HZE particles are known to deposit most of their energy localized along the path of the primary particle resulting in a dense ionization path (see Fig. 1).

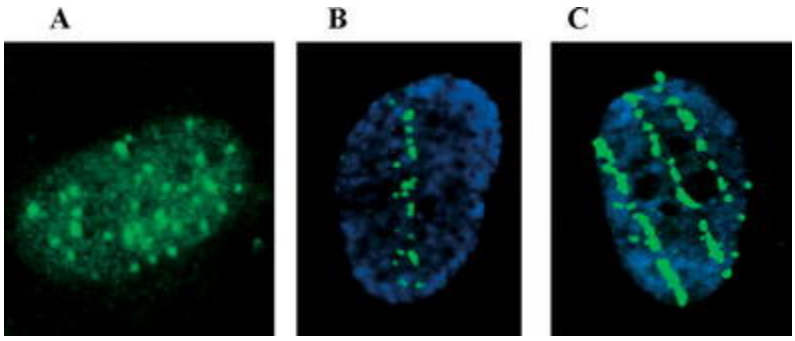

FIG. 1. Three human fibroblast nuclei irradiated with 2 Gy of γ-rays (A), 0.5 Gy of 54 keV/μm silicon ions (B) and 0.5 Gy of 176 keV/μm iron ions (C) and stained for γ-H2AX clusters. Each green spot is thought to represent a DNA double strand break (*6*).

The dense ionization caused by an HZE particle is due to its charge. Patterns of damage to DNA and mechanisms of its repair are different than for low-LET radiation (*7-10*). Although the creation of double strand breaks (DSBs) by high-LET radiation has been found to be a linear function of dose (*11-13*), it has been shown that an increased number of double strand breaks (DSBs) caused by high-LET radiation do not rejoin as easily in

comparison with low-LET radiation (*14*). There are significant gaps in the elucidation of a cell's response to high-LET radiation, and there is currently little human data examining these kinds of exposures. Current research in animals, from a limited number of studies, shows that HZE particles have an increased carcinogenic effect as compared to low-LET radiation (*15-17*). Further study is necessary to better understand the interactions of high-LET HZE particles and the resulting effects on cellular function.

Biological Response to Radiation

Radiation biology is focused on determining the nature of interactions of radiation with cells and the probability for relevant biological effects. This is fundamental for improving the reliability of health risk estimates at low doses. Several characteristics of the radiation and the target system are likely to influence the magnitude and frequency of variation in responses of individual cells. The obvious properties of the radiation are the energy deposited, mass and velocity of the charged particle, the spatial distribution of the energy deposited, and the temporal distribution of events. In experimental conditions, these variables can be characterized and defined; the biological target is usually the most difficult part of the experimental system to identify and control.

The relevant characteristics of the target system include anything that may influence the amount of energy deposited; conditions (such as oxygen concentration) that influence the consequences of energy deposition, and factors (such as cell-to-cell contact and extracellular matrix structure and the cell culture environment) that all influence the

communication of information and materials between cells. For example, the substrate, and the cell population density influence the geometry of the cell (how flattened it is), which in turn influences the energy deposited by a particle with a given stopping power. This may also influence the proximity of sensitive targets within the cell and possibly even the effectiveness of some repair processes. Cell culture is a good example of an environment in which cells will take on a more flattened geometry. Cells in this environment attach to the substrate, a cell culture flask, divide, and spread evenly across the flask. At low densities these cells have no contact inhibition and their growth is not directed by other cells. Because of this, the cells in culture must be closely monitored and passed, or split, into multiple other flasks when they have covered approximately 85% of the substrate surface. It is due to this constant growth and spreading that leads to a more flattened geometry. In contrast, cells in organized environments, such as tissue, are contact inhibited and their growth is directed by other cells. Therefore, normal cells have a defined growth cycle. In most tissues, this results in a much less flattened geometry in comparison with similar cell types cultured in flasks.

The number of cells per unit area on the dish clearly influences the opportunity for gap junction communication between cells, but it also may influence the nutritional status of the cell and signals relevant to cell cycle regulation. Experiments with monolayer cell cultures cannot fully represent the effects that may occur in normal tissues.

Normal tissue is a combination of extracellular matrix, immune system, vasculature, multiple cell types, etc., and each factor impacts a cell's response to stimuli. For example, the media used in cell culture systems is thought to sufficiently nourish the cells; however, there is not a complete understanding of what a cell needs to fully function and mimic an *in vivo* condition. In fact, media components, such as fetal bovine serum, cannot be completely characterized; hence, there is no assurance that a cell is receiving the same nutrition it would receive *in vivo*. Thus, the further from a normal tissue a cell is cultured, the more difficult it is to attribute its response solely to the stimulus. Organ cultures and reconstituted tissues are currently the best system to simulate the normal cell environment as closely as possible, and yet provide the reproducibility and flexibility needed to make it possible to interpret the results of radiation exposure.

Cell Culture Model

Cell culture models have been central in understanding the interaction of radiation and individual cells. The primary advantages of using cell culture models for radiation experiments are that they are easily manipulated and isolated. These models are important when studying complex intracellular pathways because they can be examined without disturbance by signals from other cell types or the extracellular matrix. In addition to being easily manipulated and isolated, irradiations are more reproducible with cell culture models. Microbeam experiments are very useful in radiation response

studies because the ease of targeting one cell in an environment of a larger number of adjacent cells.

The bystander effect (i.e., the response of neighboring, unirradiated cells after a single cell irradiation) is often studied using microbeams and cell cultures. There is evidence that some members of an irradiated population alter their levels of repair related proteins (*18*), and change their DNA metabolism (*19-21*) even though they cannot have been directly hit by an ionizing particle. This effect has become important as it may imply, though equivocally, that a lower dose of radiation can cause an increased response compared to the one-hit, linear no-threshold model used to estimate rates of carcinogenesis and in setting dose limits. The bystander response has been seen in multiple cell culture systems (*22-24*); however it has not been demonstrated categorically *in vivo*.

These confounding and equivocal findings demonstrate the shortcomings and disadvantages in using an *in vitro* system. There are two primary disadvantages of using *in vitro* systems. First, the cells used are often immortal, or they do not senesce. Primary cells, or cells cultured directly from tissue, are the most similar to cells found *in vivo*, but they will senesce after a few divisions making them difficult to culture. Immortalized cells seem to have some problems with growth control but maintain contact inhibition and anchorage dependency, both qualities of a normal cell type. This is important for *in vitro* studies because immortalized cells are easier to culture and make it easier to study

long-term genetic effects of radiation. Immortal cells, however, are rarely seen *in vivo* and are thought to be limited to stem cells. The second disadvantage of cell culture systems is that the cell is isolated from its normal microenvironment. A precarcinogenic phenotype seen in cells may never be seen in tissue because the surrounding cells and extracellular matrix affect the cellular response. Cells are stimulated to divide, differentiate, or self destruct depending on signals from neighboring cells and the extracellular matrix. This *in vitro* characteristic removes variables that interfere with a single cell's response, however these variables can have a significant impact on a cell's natural response to stimuli. Underlying most simple cell culture models is the assumption that the irradiated response in a monolayer of homogenous cells is the same response that would be measured in a complicated tissue system with multiple cell types and an extracellular matrix. As a result, cell culture models downplay the importance of interaction with the microenvironment to the overall response of cells.

Respiratory Cells

The tracheo-bronchial epithelium covers less than 1% of the lung surface exposed to the atmosphere but gives rise to approximately 90% of all primary lung tumors (*25*). The epithelium is a pseudo-stratified, differentiated epithelium characterized by basal, secretory and ciliated cells (see Fig. 2). Basal cells are small cells adjacent to the basement membrane and do not reach apical contact with the lumen. Traditionally, these

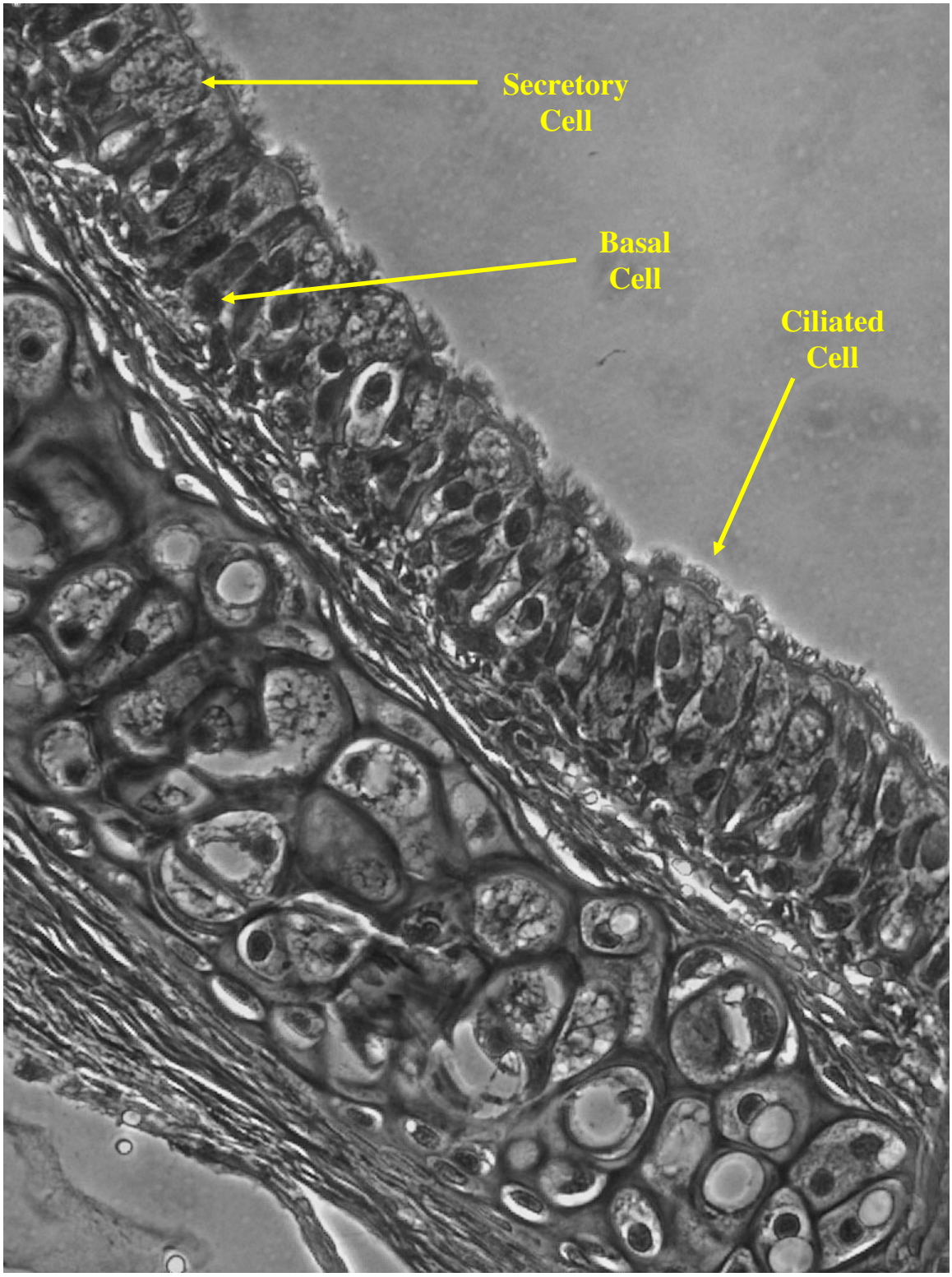

FIG. 2. A rat trachea with the secretory, basal and ciliated cells labeled.

cells are considered the stem cells of the epithelium and have been found to generate secretory and ciliated cells in rabbit trachea (*26*). Studies have also shown that less than 1% of airway epithelial cells are proliferating at any time and cycling cells are predominantly located near the basement membrane (*27, 28*).

In the trachea epithelium, secretory cells are tall, columnar cells which have apical contact with the lumen and are characterized by numerous secretory granules. Secretory cells are also able to differentiate. Following epithelial injury in hamsters, studies show that the major proliferative response at the wound edge is by the secretory cells (*29*). Basal cells and secretory cells are both able to differentiate, but their role in the repair of the trachea epithelium is not clearly understood. Ciliated cells also have apical contact with the lumen and are instrumental in moving mucus upward through the respiratory track. Ciliated cells, however, are thought to be terminally differentiated and unable to divide.

The complicated coordination of each cell type forms the tracheal epithelium and provides the primary line of defense against toxic inhalants. Most particles are efficiently removed by the cilia without harming the trachea; however, there are environmental factors that can quickly cause extensive damage to the sensitive epithelial layer before removal. Damaging factors include cigarette smoke, smog, toxic chemicals, radon exposure, etc. While cigarette smoking is the number one cause of lung cancer,

radon exposure has been estimated to be the leading cause of lung cancer in non-smokers.

Rn-222 is a naturally occurring radioactive gas found in varying concentrations throughout the United States. The gas exhausts from the soil and can accumulate in poorly ventilated homes or in ground water. Rn-222 is considered a hazard to lung tissue because it emits a high energy, 5.6 MeV, alpha particle. The alpha particle will deposit its energy in a short distance and cause localized damage to lung tissue. This damage, delivered chronically over many years, leads to fibrosis. Damage is accelerated if paired with another damaging factor (cigarette smoking) and can lead to lung cancer. Epithelial lung tissue, its sensitivity to damage and its role as a primary barrier in fending off pollutants (including ionizing radiation), makes it structure and cellular components an important model for studying radiation injury.

TGF-beta

TGF-beta is a signaling transducer stored extracellularly in its latent form and is thought to provide a reservoir for future use by preserving its inactivity through attachment to extracellular components (*30*). TGF-beta is secreted in its latent complex in two forms; the first form, small latent complex, is a dimer of the TGF-beta homodimer and the latent associated peptide (LAP); the second form, large latent complex, contains a third component, the latent TGF-beta binding protein (LTBP). Each complex is attached to a

proteoglycan, decorin or betaglycan, and is attached to the extracellular matrix or the cell surface, respectively. This proteoglycan binding preserves the inactivation of TGF-beta (see Fig. 3).

Activation of TGF-beta requires LAP to be cleaved from the TGF-beta homodimer. Once activated, TGF-beta attaches to cell surface receptor TGF-beta type II which dimerizes with TGF-beta type I receptor, resulting in the initiation of the TGF-beta pathway (*31*). The initiation of this pathway causes a cascade of intracellular events. Smads, latent gene regulatory proteins, are phosphorylated by the activated TGF-beta receptor; in this case, Smad2 or Smad3. This receptor-activated Smad disassociates with the receptor and binds to Smad4 to make a complex. This complex moves through the cell to the nucleus and activates a target gene. The activation of the TGF-beta pathway has three major roles within a cell: immunosuppression, deposition of extracellular matrix components and epithelial cell growth inhibition (*32*). TGF-beta studies have also characterized its role in radiation-induced fibrosis and carcinogenesis (*33-36*).

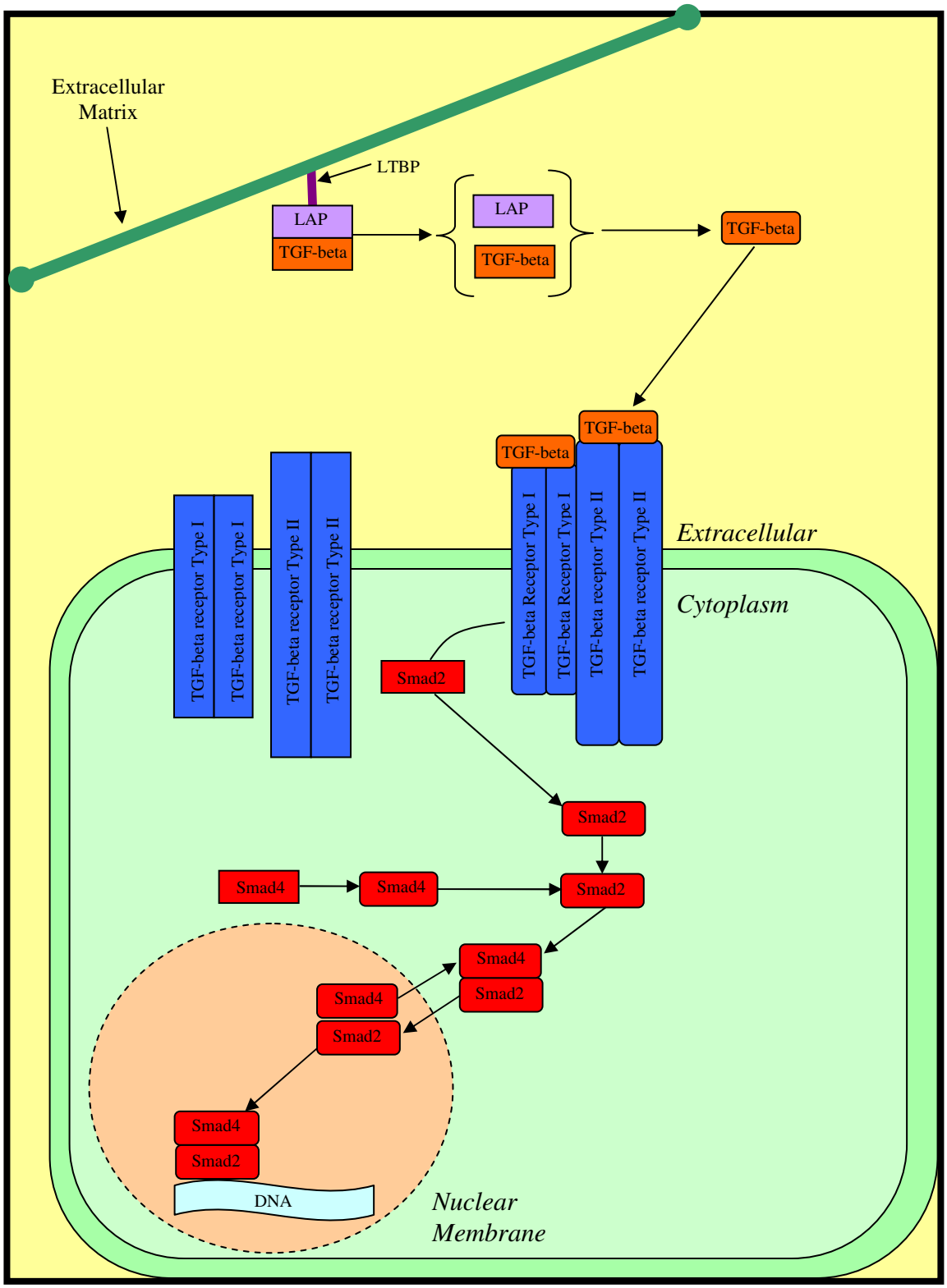

FIG. 3. TGF-beta is a coordination of intra and extracellular processes.

Fibrosis is characterized by the disorganization of the extracellular matrix and is caused by over response of the tissue to injury. Normally, a tissue will respond to injury through activation of mesenchymal fibroblasts, production of extracellular matrix components, and an organized deposition of these components (*33*). Feedback mechanisms then downregulate this response and cease the production and deposition of the extracellular matrix components. Fibrotic disease is the loss of regulation in this balanced response to injury and can lead to excessive production and deposition of extracellular matrix components, excessive tissue contraction, and the eventual loss of tissue function. Currently, there is no effective therapy for the disease and patients often must resort to organ transplantation. Examples of fibrotic diseases include liver cirrhosis, idiopathic pulmonary fibrosis, arteriosclerosis, and rheumatoid arthritis. In addition to these diseases, fibrosis is observed to be a sequel to radiation therapy. Feedback mechanisms are being investigated in order to understand what causes the over response to occur. TGF-beta, a profibrotic protein, has been shown to be a precursor to fibrosis (*33-36*).

Inhibiting TGF-beta activity has been shown to affect the composition of the extracellular matrix and play a significant role in fibrosis induction in the lungs (*37, 38*) and also affect how a cell responds to radiation (*39*). Because of its role in fibrosis, TGF-beta has been proposed to play a critical role in tissue repair after radiation injury. Specifically, Ehrhart, et al. found that blocking TGF-beta receptors with neutralizing antibodies reduced the collagen III immunoreactivity in the adipose stroma after 5 Gy

whole-body irradiation of mice (*39*). Xavier, et al. also found that the inhibition of the TGF-beta pathway results in a resistance to high dose, 35 to 45 Gy, hind leg radiation exposure and fibrosis formation in mice (*40*). TGF-beta clearly plays a role in collagen production after irradiation, but its role may not be limited to fibrosis. Studies have also found that preneoplastic transformation is influenced by the concentration of TGF-beta in one model system (*41, 42*) and TGF-beta has been implicated as a possible mediator of some reported bystander effects (*15, 43*). To what extent TGF-beta affects a cell's function may be unknown, however, its role in fibrotic disease is known to be significant and is a focus of this study.

CHAPTER II

BIOLOGICAL ASPECTS OF MODEL DESIGN*

Currently, most radiation biology research, particularly high-Z and energy (HZE) experiments, utilizes cell culture models. These cell culture models are a 2-D model consisting of a monolayer of immortalized cells cultured in a cell culture flask. There are examples of cells that are maintained in a 3-D environment because their growth does not require attachment to a matrix; though, the limitations addressed here for the 2-D model are also applicable to contact inhibited cells. The 2-D model has significant advantages for certain experiments (microbeam irradiations, intra-cell signaling pathways, those that require real-time observations, and controlling growth factors and nutrition); however most neglect the importance of the extracellular matrix and other supporting cell types on the response of a cell to stimuli. It is known that signal transduction, shape, and differentiation of a cell may be controlled by its 3-D environment (*44*). Also, cells used in 2-D experiments are often from a single cloned cell line and cannot perform all functions of a complete organ or tissue. Moreover, signaling between multiple cell types does not occur in a 2-D environment. These influences are significant, especially when trying to extrapolate monolayer cell results and *in vivo* environments.

---

* Portions of this chapter are reprinted with permission from "Radiation responses of perfused tracheal tissue" by J.R. Ford, A.J. Maslowski, R.A. Redd and L.A. Braby, 2005. *Radiation Resarch*, **164**, 487-492. Copyright 2005 by Radiation Research

Despite the importance of using tissue structures for radiation biology experiments, there are considerable experimental limitations in performing all such experiments on systems that maintain tissue matrices and mimic *in vivo* environments; nevertheless, experimental systems that are closer to this 3-D organization can be more directly compared to *in vivo* results. Attempts to emulate *in vivo* environments have been tried with success. The Whitcutt chamber, which is often used for tracheal cells, allows for epithelial cells to differentiate while maintaining an air-liquid interface (*45, 46*). Cells are grown on collagen treated porous membranes that allow for media to nourish the basal layer and the ciliated and secretory cells to maintain apical contact. This model, however, does not maintain the tracheal fibroblasts or cartilage rings. Collier, et al. also attempted to maintain the *in vivo* environment by using ring organ cultures (*47*). This design incubates trachea rings, cut transversely and having one cartilage ring intact, in Petri dishes with media. In contrast to the Whitcutt chamber, this model does maintain the fibroblasts and the cartilage rings, but it does not have an air-liquid interface. Each model offers an improvement to the widely used cell culture model, but neither is able to include significant trachea features: multiple cell layers, the cartilage rings and the liquid-air interface.

Cell behavior has been found to be determined not only by its genome, but by its microenvironment. Early experiments found that injecting carcinogenic cells into a normal tissue environment would cause the cells to revert to a normal tissue (*48*). In addition to cancerous cells reverting to a normal phenotype, studies have used mouse

mammary epithelial cells as a model to determine if normal tissue could become pre-neoplastic through the influence of the tissue microenvironment (*35, 49-51*). While a definite answer to this question remains elusive, the results further confirm the correlation between a well structured microenvironment and tissue health. If a well structured ECM is important for a healthy functioning tissue, then what effect does irradiating a tissue have on the ECM and the tissue as a whole? Barcellos-Hoff, et al. found that irradiation of mouse mammary stroma promoted neoplastic formation by altering the ECM and growth factor activities (*52*). These results are based on low-LET gamma irradiation; however, similar ECM reorganization was found after irradiating mouse mammary glands with high-LET iron particles (*53*). Therefore, it is unclear if radiation carcinogenesis is a contributing factor or the result of disrupting the tissue microenvironment. In lungs, this same disruptive reorganization is called fibrosis and is known to result from high-LET irradiation (*54*). Therefore, to investigate the radiation effects on the ECM in lungs, a previously developed *ex vivo* tracheal model has been adapted for this study.

In 1981, Gabridge and Hoglund developed a unique matrix-embedded perfusion system for guinea pig trachea (*55*) which was later used for hamster trachea (*56*). The system design allowed for an intact, *ex vivo* trachea to maintain a near normal metabolism, structure and function for a short time. After aseptically removing a guinea pig trachea, it was embedded in an agar matrix and placed in a Teflon® block. The Teflon® block was manufactured with a well on each end with a narrow canal, where the trachea would

be embedded, connecting the two (see Fig. 4). The design allowed for media to flow from well to well through the tracheal lumen while gently washing the trachea with nutrient rich media.

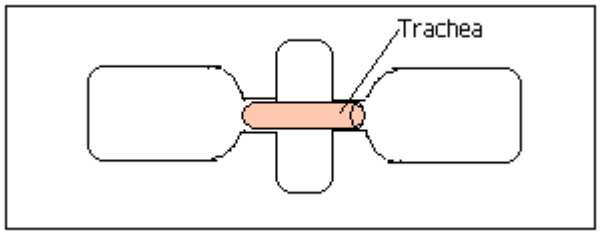

FIG. 4. Diagram of the perfusion chamber designed by Gabridge and Hoglund. Adapted from Gabridge and Hoglund, 1981 (*55, 56*).

While this perfusion chamber design was useful for experiments researching the effects of chemical toxins, the Teflon® block limited the use of the perfusion chamber in radiation experiments; therefore, its design was modified to limit the shielding of the radiation by the supporting block.

The Teflon® block was redesigned for this research; however, the basic concept of the perfusion chamber, i.e., the flow of media through the tracheal lumen, was retained. Based on the expectation of having multiple trachea samples for irradiation, we chose a commercially available cover slip well as our container (see Fig. 5). This design allowed for all the benefits of the original perfusion chamber's original design while reducing the shielding of the trachea. The reduced shielding was an important

characteristic for the experiment because we wanted to ensure the accelerator and x-ray irradiations delivered the dose determined by the dosimetry measurements. This helped to reduce the uncertainty of the irradiations.

FIG. 5. Pictured is a perfusion chamber with a nearly full length (~2cm) trachea that was cast in an agarose block.

Tracheal Epithelium Repopulation

The goal of establishing a perfusion chamber system, which would maintain a trachea *ex vivo*, was to establish another bridge between cellular and *in vivo* models. Currently, xenografts serve as the primary example of a model that maintains the extracellular environment, multiple cell types, and is used to connect cellular and *in vivo* model results. Xenografts are used for multiple organs, but are particularly well suited for trachea experiments.

Rat tracheal xenografts are tracheas which have been excised and subcutaneously transplanted in a host animal. The host animal accepts the graft, develops a vascularization system to the trachea, and the viability of the trachea is maintained in the host. This model has been used to determine the effects of carcinogens on rat tracheal epithelial cells by placing a pellet of carcinogenic material in the trachea prior to transplantation (*57*). Further research has shown that excised, denuded tracheas can be repopulated with epithelial cells, transplanted subcutaneously in rats, and exposed to carcinogens (*57, 58*). Denuded trachea provided the basal lamina architecture necessary for extrinsic epithelial cells to attach, differentiate, and reconstitute the epithelium. The success of repopulating denuded trachea suggested the possibility of repopulating denuded trachea with human epithelial cells.

Experiments using human cells to repopulate denuded rat tracheas have been achieved (*59-61*). This success provided another step in the bridge connecting animal data to human data. This is a step we wanted to achieve to more closely relate the results of the perfusion chamber system to human cells. This would be attempted by repopulating a denuded trachea with human bronchial epithelial cells using the perfusion chamber model.

Materials and Methods

Animals

Young adult male Fischer 344 (~300 g) rats (Harlan, Indianapolis, IN) were housed in approved animal facilities and tracheal tissue was harvested using methods approved by the institutional Animal Care Committees of Texas A&M University and Brookhaven National Laboratory, and conformed to NIH guidelines.

Tissue harvest

To obtain tracheas for perfusion cultures a wide anterior thoracotomy was performed under terminal anesthesia. Terminal anesthesia was accomplished by intraperitoneal (IP) injection of sodium pentobarbital at a dose of 140 mg/kg. After exposure of the anterior mediastinum under strict aseptic conditions, the tracheas were separated from the surrounding tissues by blunt dissection. The tracheas were freed by cutting just above the bifurcation and below the larynx. The tracheas were stored for several hours on ice in complete medium while the chambers were prepared.

Media

The media for the perfusion chamber trachea was made of two sets of ingredients. The first, B1, was used for primary epithelial cell repopulation experiments. B1 was prepared at two times the necessary growth factor concentration, and consisted of the following components and concentrations: Ham's F-12 (95%, Gibco, Grand Island, NY), Epidermal Growth Factor (0.004%, Gibco, Grand Island, NY), gentamicin (0.2%, Gibco,

Grand Island, NY), hydrocortisone (0.02%, Gibco, Grand Island, NY), insulin (0.1%, Gibco, Grand Island, NY), and Fetal Bovine Serum (5.0%, Gibco, Grand Island, NY). Media used for normal human bronchial epithelial repopulation experiments, BEGM, was also prepared with two times the necessary growth factor concentration and consisted of the following components and concentrations: Ham's F-12 (92.8%, Cambrex, Walkersville, MD), Fetal Bovine Serum (5%, Gibco, Grand Island, NY), Human Epidermal Growth Factor (0.2%, Gibco, Grand Island, NY), gentamicin (0.2%, Gibco, Grand Island, NY), hydrocortisone (0.2%, Gibco, Grand Island, NY), insulin (0.2%, Gibco, Grand Island, NY), transferrin (0.2%, Gibco, Grand Island, NY), Bovine Pituitary Extract (0.8%, Gibco, Grand Island, NY), epinephrine (0.2%, Gibco, Grand Island, NY), triiodothyronine (0.2%, Gibco, Grand Island, NY).

Perfusion chambers

Tracheal perfusion chambers were made using a modification of the techniques of Gabridge and Hoglund (*55*) and Marcus and Baker (*56*). The tracheas were trimmed to remove any rough edges and were placed into the chambered coverglass wells (Lab-Tek, Naperville, IL) that were used as perfusion chambers (Fig. 6). Medium (*62*) made with twice the normal quantities of growth factors (2X) was mixed with 3% agarose in equal quantities. This agarose mixture was poured over the trachea placed in the perfusion chamber and placed in the refrigerator to harden. Once the agarose mixture hardened the trachea was rinsed with medium to insure that the lumen was clear and free flowing. The medium reservoir that remained on either side of the trachea was filled with a

minimal volume of medium and the chamber was placed on an oscillating table. The gentle rocking motion insured that the entire tissue sample was periodically washed with medium providing nourishment, while still providing air exposure. Washing of the tracheal lumen occurred every seven seconds, or approximately eight times per minute.

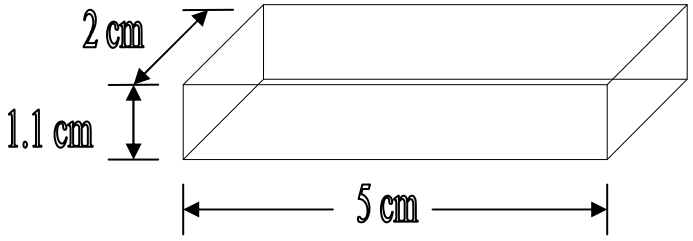

FIG. 6. Diagramed is a Lab-Tek® chambered coverglass well with dimensions: 5cm x 2cm x 1.1cm. The coverglass well is used for the adapted perfusion chamber.

Tracheas were denuded by incubating on the rocker for 30 minutes using 1.0% of Triton-X 100 (Sigma, St. Louis, MO). After incubation, the trachea's lumen was rinsed with BEGM media until no visible cells were flaking off. This treatment prepared the trachea for repopulation with suspension of primary culture cells.

Cells

Cells used to repopulate the denuded trachea came from primary tracheal cell cultures or an established human bronchial epithelial cell line. Primary tracheal epithelial cells were obtained as follows. Tracheas freshly removed were cut through the ventral rings, and filled with 1% pronase (Sigma, St. Louis, MO) in Hanks' buffered saline solution

(Gibco, Grand Island, NY) and were incubated for 18.5 hours at 4°C. After incubation, cells were removed by repeated flushing of the lumen with 10 mL of cold B1 media. Cells from three to five tracheas were pooled, centrifuged for 10 minutes at 800 rpm, and the supernatant was then removed. The cells were resuspended in B1 media with 1 mL of DNAse and allowed to sit at room temperature for five to ten minutes. The cell suspension was then passed through a 5 mL pipette ten times, a 19 gauge needle by syringe 20 times, and then passed to a 27 gauge needle by syringe. The cells were then suspended in medium and seeded. The other cell line, normal human bronchial epithelial cells (CC-2541, Cambrex, West Chester, PA), was removed from cryopreservation and resuspended using BEGM media. The nHBEC's were plated in 25 cm^2 flasks with BEGM media at a density of 10,000 cells/cm^2. When the cells were needed for repopulation experiments, 3 mL of trypsin was added for five minutes. After five minutes, 6 mL of trypsin neutralizing solution was added and the cells were centrifuged at 800 rpm for five minutes. The supernatant was removed, the cells resuspended in 10 mL of BEGM, and the cells were ready for repopulation experiments.

Tissue staining

Formalin-fixed tracheal sections were examined using propidium iodide (0.5 µg/mL, Molecular Probes, Eugene, OR) to aid identification of cell nuclei and PCNA antibodies (1:100 in 5% normal horse serum, Zymed Laboratories Inc., San Francisco, CA) to aid identification of cycling cells and DNA repair. The samples were coverslipped with a commercially available anti-fade agent (Vector) and stored in a refrigerator until viewed

with the Axiovert 200M microscope (Carl Zeiss, Thornwood, NY). Three samples were used for each data time point, and there were twelve fields, corresponding to approximately 200 µm, for each trachea sample.

Results

Comparison of tracheal cell density and apoptotic index versus time in perfusion chamber

To determine the viability of the tracheal samples maintained in the coverglass wells, we investigated the number of apoptotic bodies in the trachea over time. It was found that the number of epithelial apoptotic bodies remained constant for one and three days, however, there was a large increase at day seven (Fig. 7). Further analysis of the epithelial layer condition was required due to the large increase of apoptotic bodies at day seven. Therefore, tracheal tissue was stained with propidium iodide and viewed using a fluorescent microscope.

Inspection of the stained tracheal tissue after seven days in the perfusion chamber found that the epithelial layer loses cell density as compared to one day in the perfusion chamber (Fig. 8). Due to the reduction in cell density and the increase of apoptotic bodies, the tracheal irradiations were planned to occur within 24 hours of placement in the perfusion chamber, and the trachea did not remain longer than three days in the perfusion chamber before fixation.

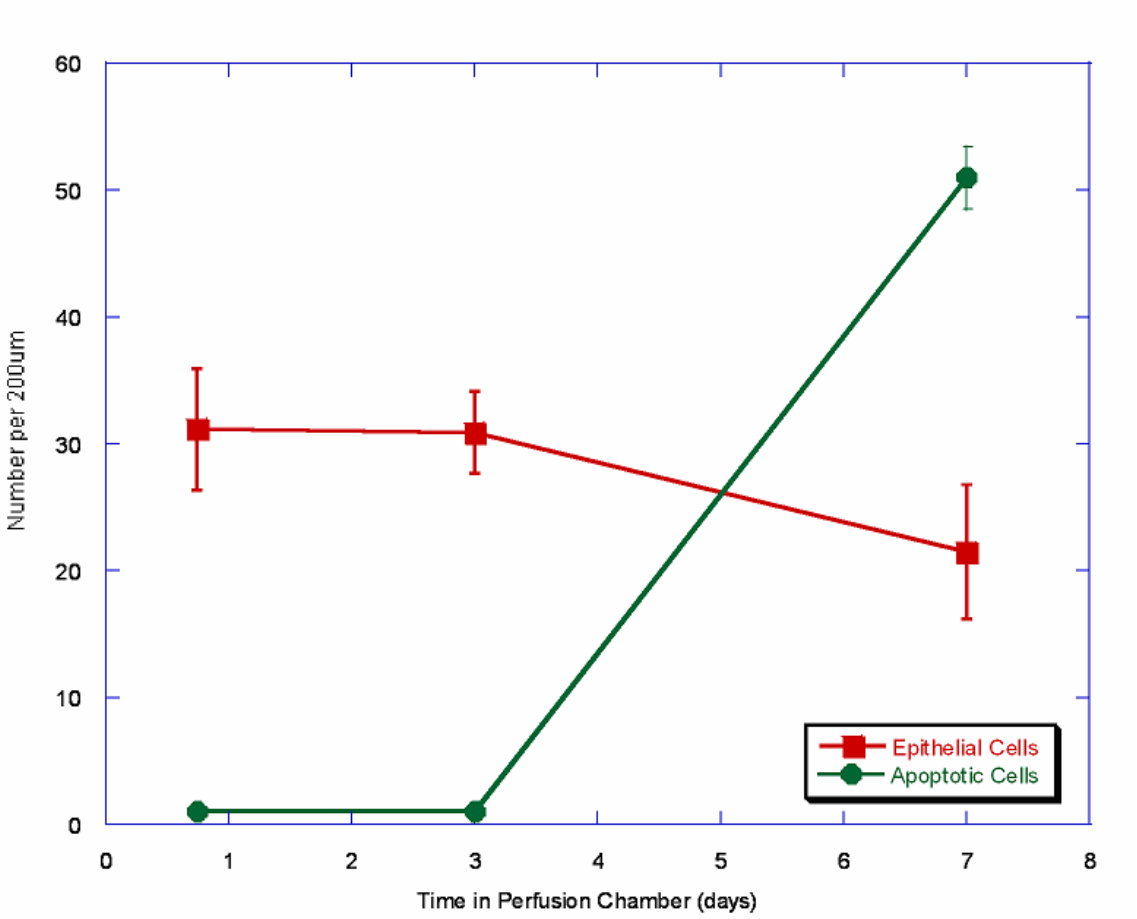

FIG. 7. Cell density and number of apoptotic bodies compared to time in perfusion culture.

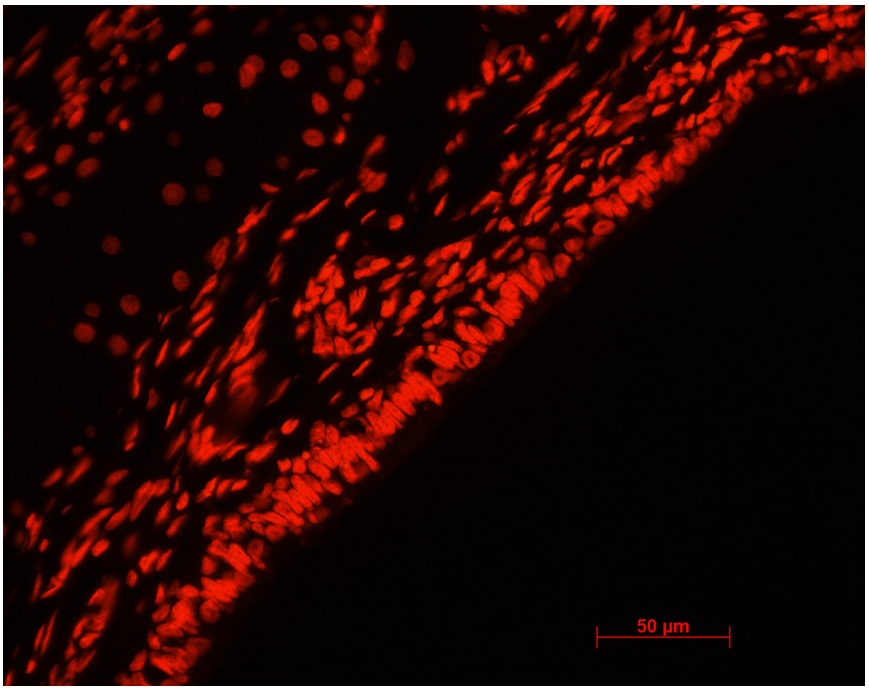

A

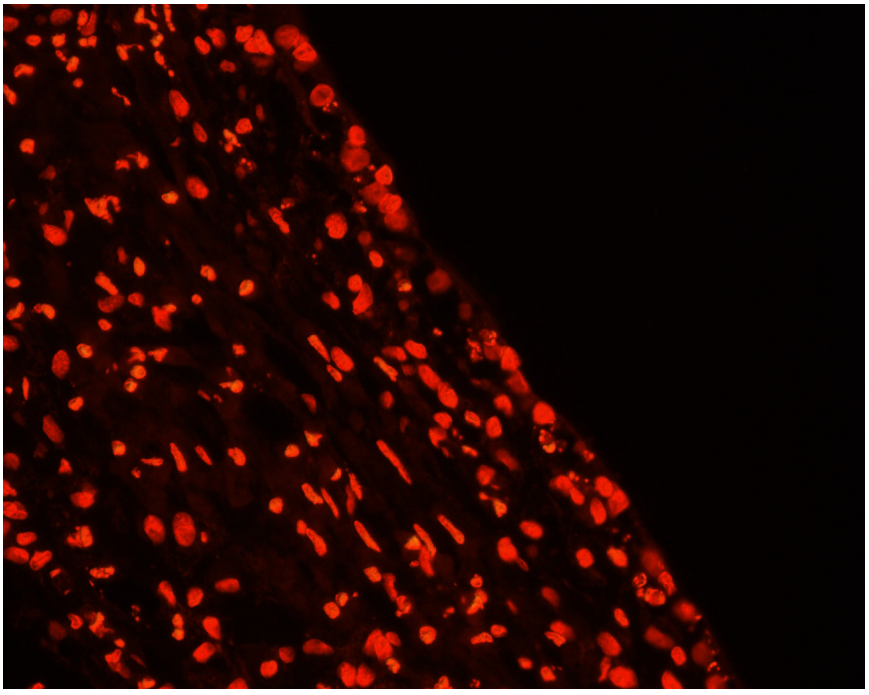

B

FIG. 8. Propidium iodide stained trachea after 18 hours (A) and seven days (B). There is a reduction in cell density of the epithelial layer at seven days in the perfusion chamber as compared to 18 hours in the perfusion chamber.

Apoptotic index versus position in perfusion chamber

The apoptotic index versus region of the trachea was also measured in an effort to determine why the large increase occurred at day seven (see Fig. 9). It was determined that passing the media across the bottom of the trachea, as it sat in the perfusion chamber, caused physical damage to the bottom of the trachea over time; thus, there was an increase in the apoptotic damage in this area. Correspondingly, the tracheas were found to have a very low apoptotic index at the top of the perfusion chamber trachea.

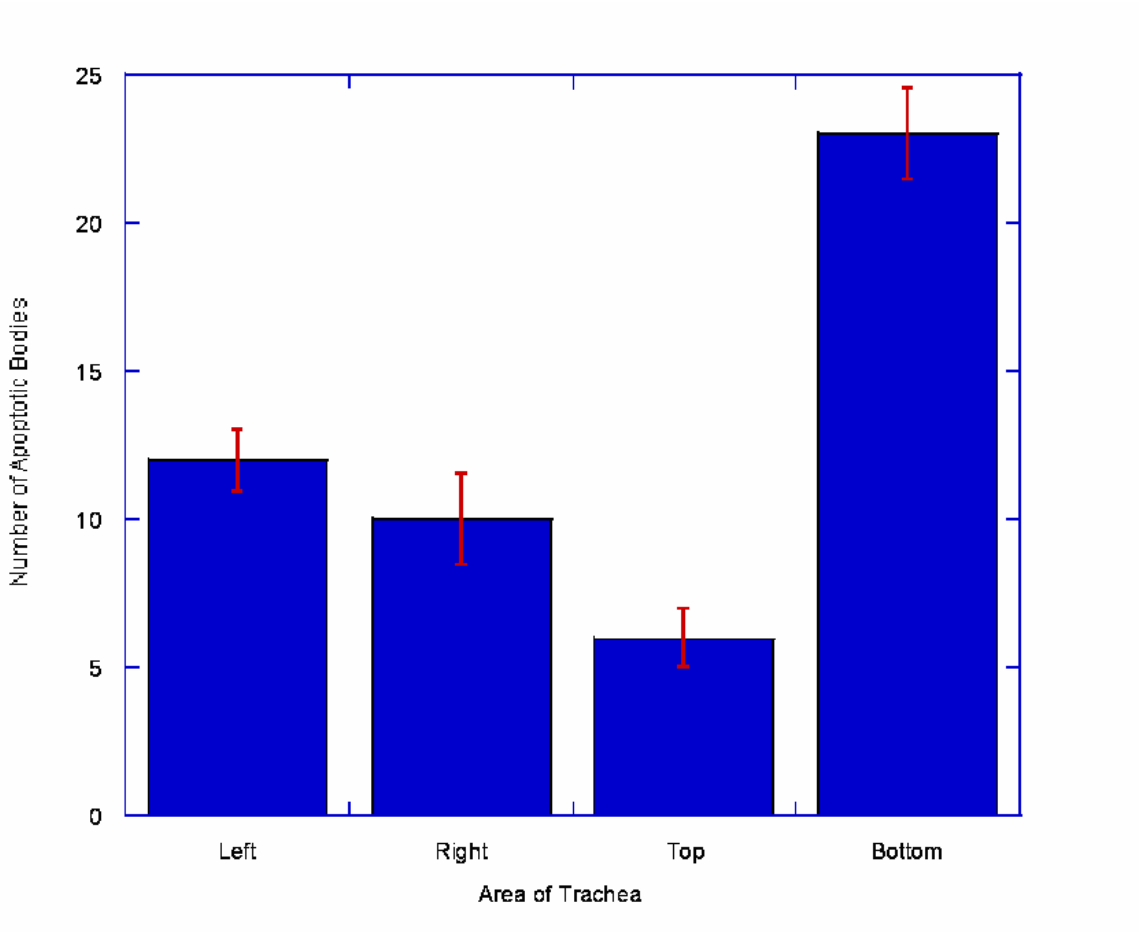

FIG. 9. The number of apoptotic bodies in different regions of the trachea maintained in a perfusion chamber for seven days.

PCNA levels versus time in perfusion chamber

Proliferating cell nuclear antigen (PCNA) is a sliding DNA clamp that is found at sites of DNA repair and replication. Due to its role, PCNA is often used to identify if a cell is undergoing high levels of repair or replication (*63*). In this experiment, PCNA antibodies were used to ensure that tracheas maintained in the coverglass wells were not showing disproportionate PCNA levels as compared to fresh trachea. Figure 10 shows the PCNA levels for the one-day perfusion chamber trachea increase as compared to the fresh trachea; however, there are no substantial increases for day three and seven. In addition, the standard deviation between day three and the fresh trachea is not significant.

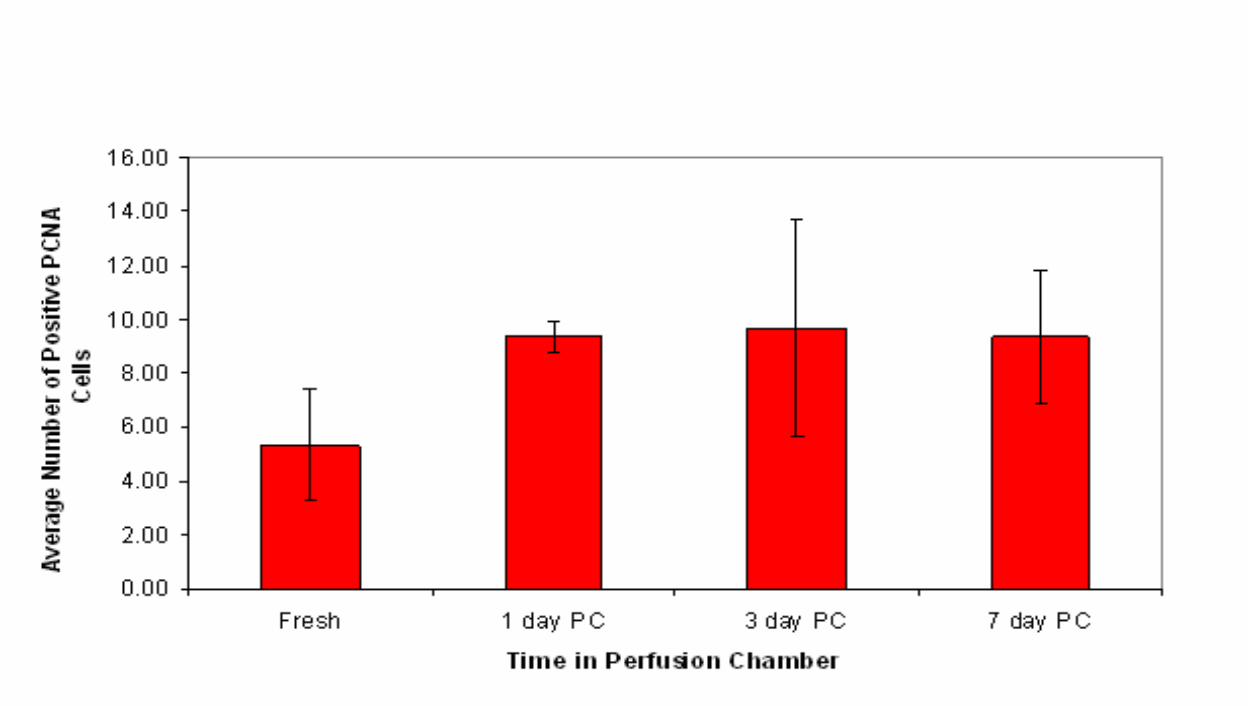

FIG. 10. Average number of PCNA positive cells as compared to time in perfusion chamber.

These results show that tracheal cells maintained in the coverglass well are not undergoing significant increases in DNA repair and replication. This is an important result because it indicates the perfusion chamber tracheas are maintaining normal physiology and monitoring damage after irradiation may be possible.

Repopulated trachea with human cells

Repopulation of denuded trachea is a technique that has been used to test carcinogens on human tracheal epithelial cells in xenografts. The success of this model has allowed for a closer connection between human and cellular data. In an attempt to provide another model, which could be used to relate human and cellular data, we investigated if denuded trachea maintained in a perfusion chamber could reconstitute the epithelium. The results indicate that the trachea could be successfully denuded of the epithelium (Fig. 11); however, attempts to repopulate the trachea with human bronchial epithelial cells were unsuccessful (Fig. 12). It was thought that the repopulation would be more successful if epithelial cells, harvested from primary trachea, were used instead. This attempt at repopulating the trachea was also unsuccessful (Fig. 13).

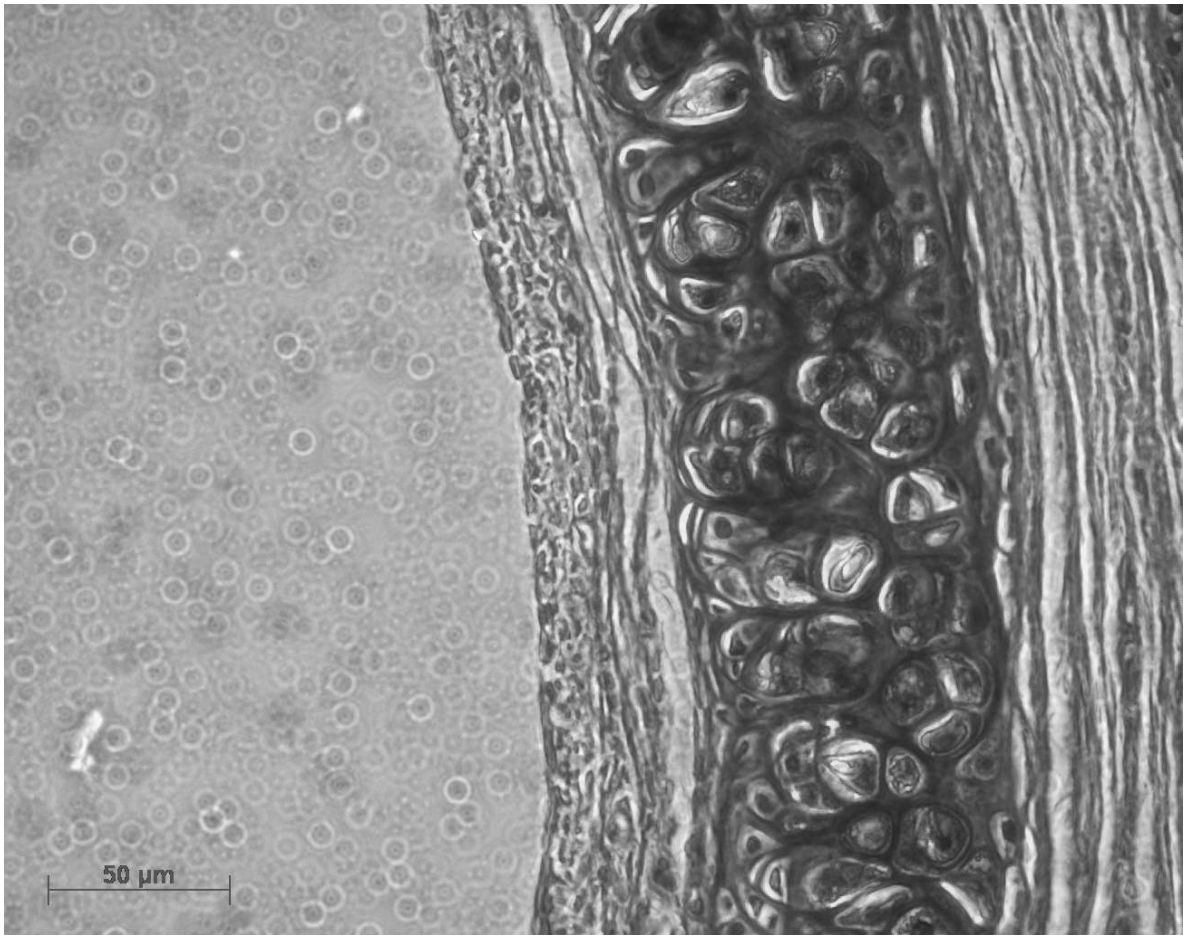

FIG. 11. Triton-X 100 denuded rat trachea image.

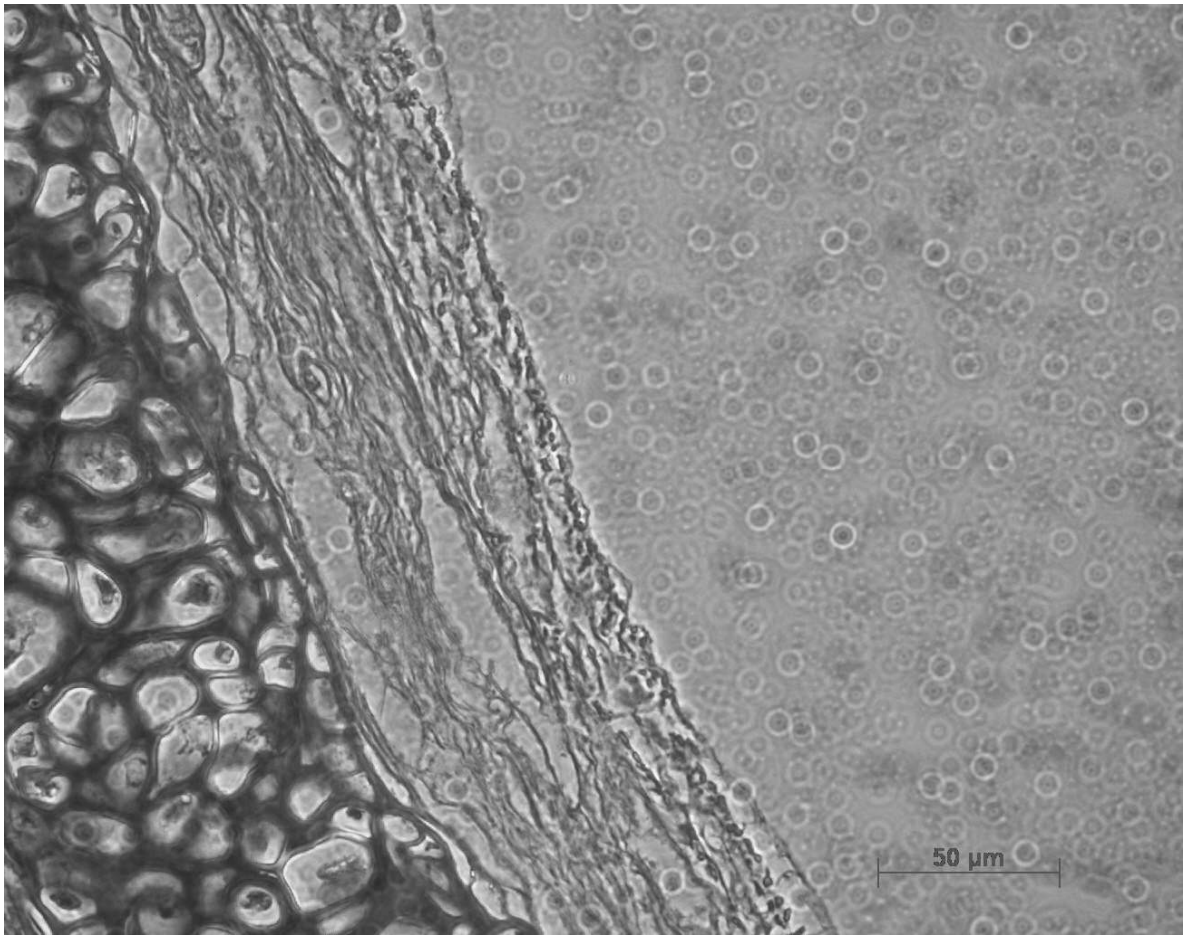

FIG. 12. A repopulated rat trachea with normal human bronchial epithelial cells.

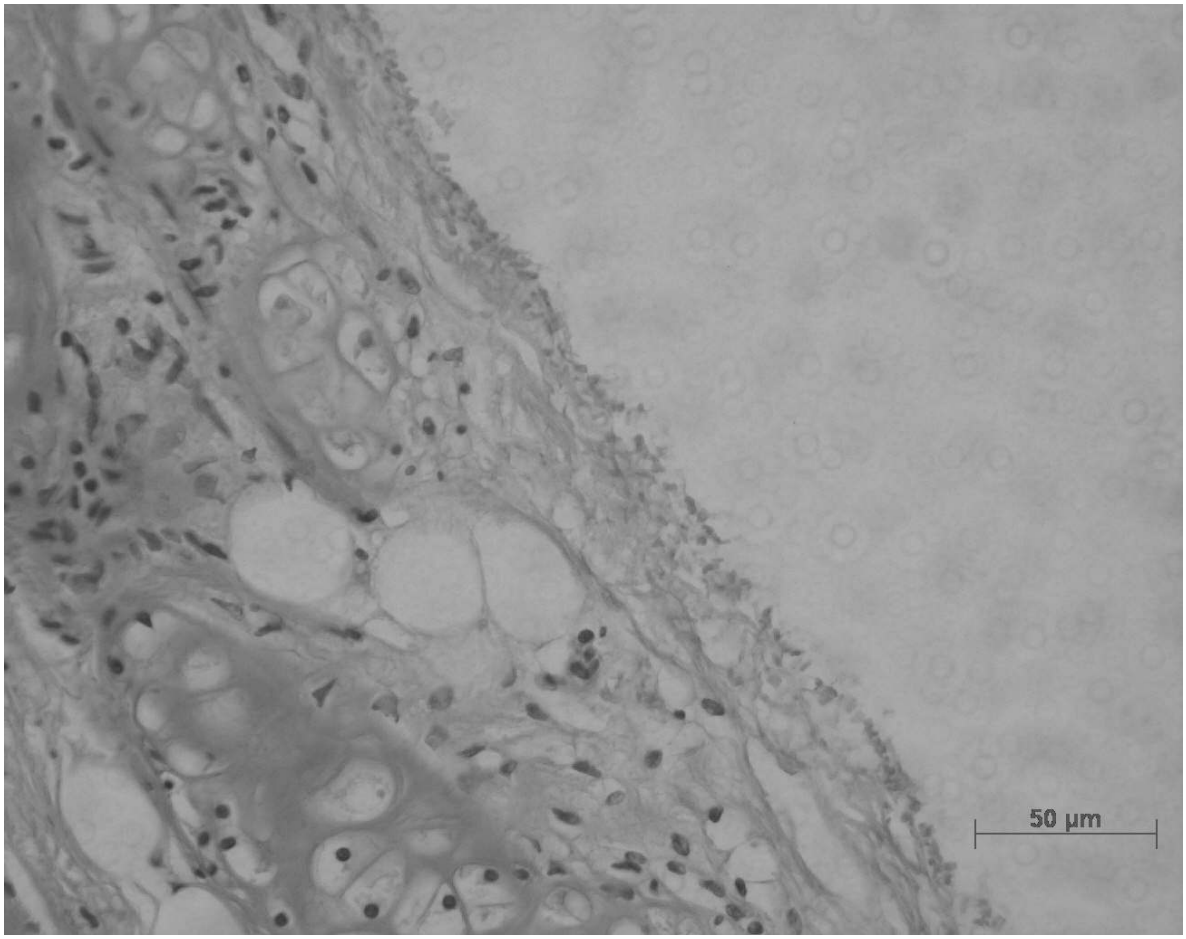

FIG. 13. A repopulated rat trachea with primary rat tracheal epithelial cells.

The perfusion chamber model relies on the washing of the trachea's lumen with media, by the rocking of the perfusion chamber, to nourish the tissue. Therefore, with each washing of the lumen, there is a possibility of washing out introduced cells. Thus, this technique is not conducive to the attachment of cells in suspension introduced into the lumen of a perfusion chamber trachea. In the xenograft model, sutures close each end of the trachea prior to transplantation into the host animal. This allows for all carcinogens, and extrinsic cells introduced, to remain within the lumen. This was not a possibility in

our model; consequently, we were not able to repopulate the denuded, perfusion chamber trachea with new cells.

Discussion

The adaptation of the original perfusion chamber design by Gabridge and Hoglund as well as Marcus and Baker for irradiation of rat tracheal tissue was successfully demonstrated. After analysis of propidium iodide staining, physical damage to the epithelium, and PCNA antibody reaction, it was determined that the coverglass well maintains the tracheal tissue in acceptable condition for up to three days. After three days, the trachea began to exhibit increased stress and damage to its physiology and morphology. Therefore, in order to ensure experiments using perfusion chambers were performed at the peak of the trachea's viability, irradiation experiments were to be performed within the first 24 hours and to remain in the perfusion chamber less than 72 hours. Performing experiments outside of this window would introduce increased variability into the experiment and we did not expect it to provide significant results with the increased time.

In addition to ensuring viability, it was necessary to adapt the original perfusion chamber design materials to commercially available ones. The material previously used was not suitable to our irradiations due its thickness and density. Due to its minimal thickness, the new coverglass wells would not excessively shield the trachea or cause extreme

scattering of the ion beam before reaching the trachea. This material characteristic was important to ensure that the dosimetry measurements for the accelerator and x-ray irradiations were consistent. The standard coverglass well helped reduced variability in the irradiations as well as between perfusion chamber preparations.

The nature of working with tissue explants in experimental models introduces numerous variables (multiple cell types, cartilage rings, increased cell-cell signaling, uncontrollable growth factors, nutrition needs) due solely to its structure. In an effort to reduce these, a consistent perfusion system based on commercially available materials was designed and tested. After analysis of the trachea response (apoptotic bodies, PCNA response, and physical damage to the epithelium), it was found the trachea was viable up to three days in the perfusion chamber system. Based on these results, the perfusion chamber model was used for the following radiation response experiments.

CHAPTER III

GENE EXPRESSION ASPECTS OF MODEL DESIGN

Underlying any argument for the use of a linear extrapolation to obtain the risk resulting from low doses of radiation is the assumption that the adverse effect is the result of an individual cell acting autonomously. Single particle microbeam irradiation has shown that at least some biological endpoints can be produced by passage of a single alpha particle through a cell (*64*). There is adequate evidence that the health effect of greatest concern, cancer, is the result of the abnormal growth of a single cell. It is also known that, under normal circumstances, cells are influenced in many ways by their local environment. Cells are stimulated to divide, differentiate, or self-destruct depending on signals from neighboring cells and the extracellular matrix. There is also evidence that some members of an irradiated population alter their levels of repair related proteins (*65*), and change their DNA metabolism (*22, 66, 67*), even though they could not have been directly hit by an ionizing particle. This strongly suggests that cells do not act autonomously, and it may be that interactions between hit and unhit cells influence the probability of adverse effects in ways that depend on the number of hit cells in the population, that is, in a dose-dependent way (*18-21*). A nonlinear, dose-dependent modification of the probability of expressing radiation damage would clearly result in a nonlinear response at low doses. The problem for radiation biology is to determine the nature of this interaction and the probability for relevant biological effects, and thus provide data for improving the reliability of health risk estimates at low doses.

Several characteristics of the radiation and the target system are likely to influence the magnitude and frequency of modifications to the response of individual cells. The obvious properties of the radiation are the energy deposited, mass and velocity of the charged particle, the spatial distribution of the charged particle tracks, and the temporal distribution of events.

The rat tracheal epithelial cell culture/*ex vivo* model system enables us to examine effects in the tissue directly under culture conditions that more closely resemble the environment that respiratory epithelial cells encounter in the animal. The rat tracheal epithelial cell system has been well characterized for a large number of different endpoints (*68-70*). Preneoplastic transformation is influenced by the concentration of TGF-beta in this system (*41, 42*) and TGF-beta has been implicated as a possible mediator of some reported bystander effects (*19, 43*). The rat tracheal epithelial cells exhibit extensive gap-junction mediated, cell-cell communication in culture and in the tissue. Neoplastic progression in this system is also correlated with changes in cell-cell communication (*71*). Gap junction communication has been suggested in a number of bystander effects (*72*). Interactions between stromal cells and epithelial cells are known to be important in some tissue models of carcinogenesis and have been suggested as important factors in bystander effects and genomic instability (*19*). All of these types of interactions can be quantified in the rat tracheal system. In the evaluation of risk it is important to know the probability that an initiated cell will progress to neoplasia and the rat tracheal system has been used to examine the interactions between altered (initiated,

preneoplastic or tumorigenic) cells and normal unaltered cells (*73*). Studies have also been performed comparing the response of intact tracheal transplants and cells in culture for a wide variety of radiations and carcinogens.

In this chapter the effects of radiation on gene expression in perfusion cultures of rat tracheal sections is examined. This new culture system takes advantage of the previous information obtained with primary tracheal epithelial cells in monolayers and paves the way for microbeam or low fluence ion irradiation of thin tissue sections. By controlling the spatial and temporal distribution of dose in a model system that closely approximates the normal tissue milieu, we can quantify any adverse or beneficial bystander effects due to radiation.

Materials and Methods

The materials and methods used for the housing of animals, harvesting tissue, and perfusion chamber preparation for the following experiments are as described in Chapter II.

Chamber irradiation

Chambers were irradiated with either x-rays (250 kVp and 10 mA delivered at 1 Gy/min at Texas A&M) or placed parallel (or perpendicular) to the beam of the Alternating Gradient Synchrotron (1 Gev/nucleon iron ions, delivered at 0.5 Gy/min). Chambers received 4 Gy of x-rays or either 0.05 Gy or 0.1 Gy of iron ions. Sham exposures were

carried out for both types of exposure by placing the chambers in the irradiation position for the same time period without energizing the beams.

Immunohistochemistry

Formalin fixed tracheal sections were examined using mouse monoclonal antibodies to PCNA (Zymed, South San Francisco, CA). Samples were blocked with horse serum for an hour and then treated with the specific monoclonal antibody for one hour. Secondary antibodies (horse anti-mouse) conjugated to fluorescein isothiocyanate (Vector, Burlingame, CA) were added after repeated rinsing and left to incubate for an hour at room temperature. After repeated rinsing the samples were counterstained with propidium iodide (0.5 µg/mL, Molecular Probes, Eugene, OR) to aid identification of the cell nuclei. The samples were coverslipped with a commercially available anti-fade agent (Vector) and stored in a refrigerator until viewed with the Axiovert 200M microscope (Carl Zeiss, Thornwood, NY).

Results

Comparison of tissue maintained in perfusion chambers to freshly harvested tissue.

From preliminary experiments we had determined that an intact epithelium could be maintained for several days. Measurements of proliferative index, apoptotic index, cell number, and relative proportions of basal cells to ciliated and secretory cells were not significantly different for the first week of culture (see Chapter II). Although we knew the cells were present (Fig. 14) and appeared healthy by these measures, we wanted to

determine if cell behavior as characterized by gene expression were identical to normal tissue freshly harvested from the animals.

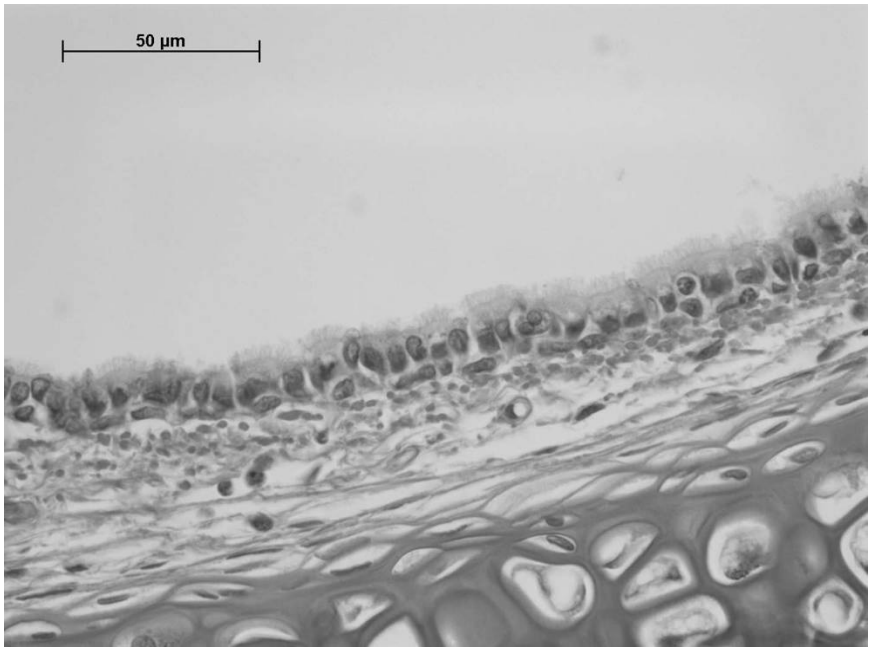

FIG. 14. Histology section from a 1-day-old perfusion chamber (H&E-stained section, bright-field, 63X objective) from the set that was exposed to iron ions at Brookhaven National Laboratory.

Changes in gene expression

Arrays were analyzed for mRNA obtained from three tracheas maintained for 24 hours in perfusion culture (sham exposed) and for three age-matched freshly harvested tracheas (one array for each sample for a total of six arrays). A total of 1718 of the sequences were judged to be under expressed; that is, the intensity of the signal from the samples obtained from perfusion chambers was less than half the value detected for freshly harvested samples. Another 891 sequences were judged to be over expressed

(more than twice the intensity) in the perfusion culture samples while the remaining 7212 sequences demonstrated no significant differences (Fig. 15).

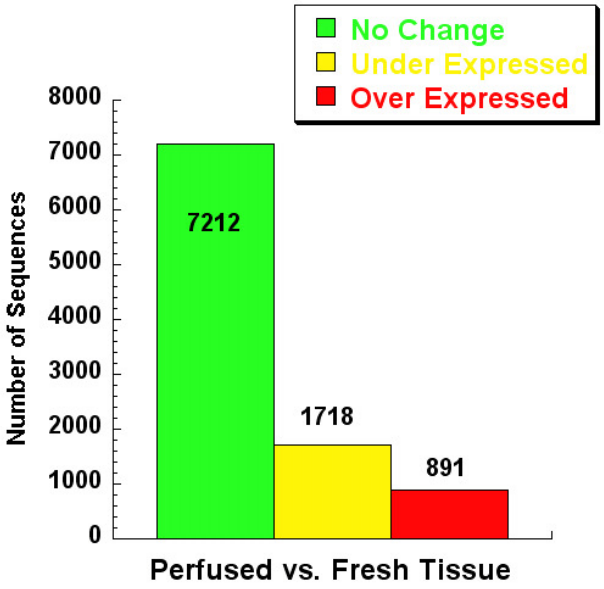

FIG. 15. Genes (or ESTs) that remained unchanged, were overexpressed (≥two times), or were underexpresseed (≤0.5) in perfusion chamber samples compared to freshly harvested trachea.

After excluding unknown sequences, the most striking over expressions were in genes associated with mucus production and secretion. In particular lipocalin (80X) and surfactant associated protein (30X), were the most expressed genes in the perfused tissue. Examination of genes associated with apoptosis, hypoxia, cell-cycle control, inflammation, TGF-beta, and stress pathways (determined by using the databases available through PubMed, http://www.ncbi.nlm.nih.gov/entrez/query.fcgi) were not significantly different, in keeping with our general histological observations. Further

analysis of the gene expression in perfused trachea can be found in Ford, et al. (*62*).

Discussion

Previous observations using the rat tracheal epithelial cell system demonstrated that, regardless of whether cells were irradiated as a single-cell suspension or in the trachea and then introduced immediately into primary culture, the same survival dose response would be obtained for a particular type of radiation (*74*). When these experiments were originally conceived, it was with the expectation that perfused tracheal sections irradiated with a low fluence of ions would demonstrate the same bystander effects observed for primary cells in culture. Instead of the expected 25-30% of the irradiated epithelial cells exhibiting detergent resistant PCNA less than 1% of the cells were PCNA+. The lack of an observable change in the fraction of cells exhibiting detergent-resistant PCNA led to an examination of gene expression profiles to begin to define possible differences that might be responsible for this result. Since the main purpose of this research was to determine the degree to which bystander effects play a role in the risk of cancer in respiratory tissue, it was necessary to study the differences between perfused tissue and freshly harvested tissue. In general, the answer was that the gene expression was not significantly different for most sequences examined (Fig. 15). Those changes that detected were mainly due to increases in genes connected to mucus secretion. This indicated that the gently rocking used to keep the tissue moist is probably stimulating mucus secretion and is not as gentle as first thought. Whether the stimulation of ciliated and secretory cells might perturb a response to radiation will

require further investigation.

One well known gene did exhibit the expected increase in expression following irradiation. Although CDKN1A expression had increased eight-fold, it did not show as dramatic an increase as might have been expected from experiments with cell lines (*75*). Most of the other sequences examined showed no difference but the samples were obtained just two hours post-irradiation. The effects were studied early because there was concern that cell loss to the medium would skew the mRNA distribution in favor of surviving cells and because bystander or adaptive responses occur within a few hours. This led to consideration of another possibility that might also affect the ability to monitor gene expression. There are three distinct cell types that make up the pseudostratified epithelial lining of the trachea. The basal cells are the only cells which can proliferate and the other two cell-types (ciliated and secretory) have specialized functions that require the expression of distinct sets of genes. This is illustrated in Fig. 16 where the staining for PCNA is restricted to a few cells of the basal layer.

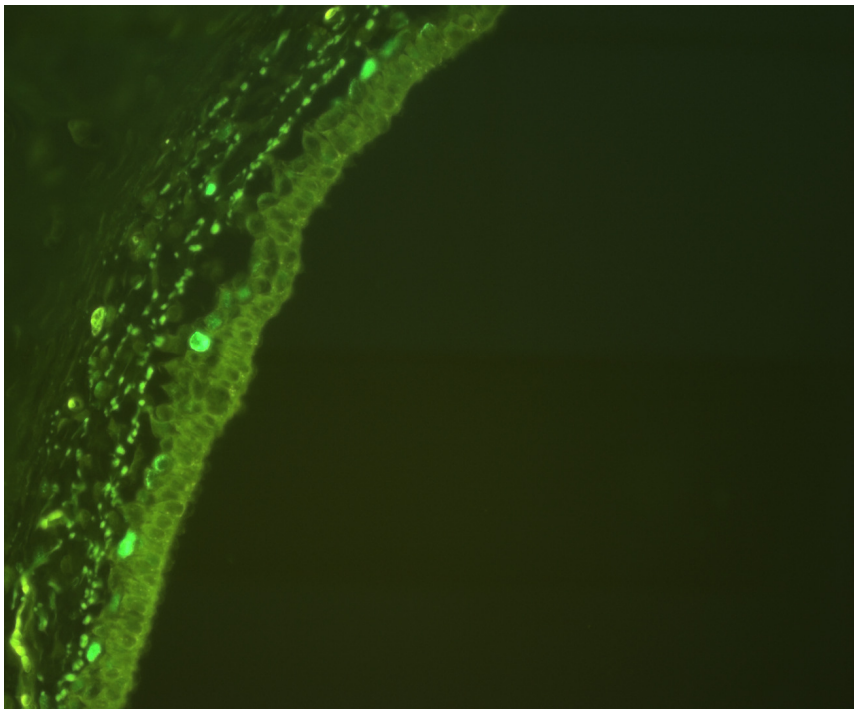

FIG. 16. One-day-old perfusion chamber treated with anti-PCNA antibody to visualize detergent insoluable PCNA. The cycling cells are restricted to the basal cell layer (at the same magnification as in Fig. 14).

In cell culture, it has been shown that it is the basal cells that act as clonogens in primary culture (*76*). Therefore, it is proposed that terminally differentiated cells do not respond to irradiation and that only a small fraction of cells, the tissue stem cells, will respond by changes in gene expression and that the presence of the other cell types dilutes the increased expression in responding cells. In the future, this hypothesis will be tested by separating the different cell types and examining the gene expression in different cell fractions. Based on these results, it is expected that the cell-cycle arrest and possibly repair genes will be over-expressed in the basal cells while they would remain relatively unchanged, if expressed at all, in the ciliated and secretory cells. The possibility that a

significant proportion of cells may not respond markedly to irradiation, or respond differently, could also explain some of the differences that have been reported in the effect of different types of radiation on tumorigenesis in the rat tracheal system (*77*).

CHAPTER IV

COMPARATIVE EFFECTS OF LOW-LET AND HIGH-LET ON THE TGF-BETA RESPONSE OF TISSUE

The radiation environment in space is dominated by two sources: galactic cosmic rays (GCR) and solar particle events (SPE). GCR are ubiquitous and isotropic and SPE are irregular and unpredictable; however, neither source is easily shielded. As a result of these sources, the radiation environment in space consists of a multitude of radiation types including: electrons, protons, positrons, neutrons, alpha particles, fission fragments, hydrogen, helium, carbon, neon, oxygen, silicon, and iron ions. These particles can range in energy from 10 MeV/n to 10 GeV/n. It is because of this mixed field of high-LET and low-LET radiation that it is difficult to shield astronauts from solar events or during extended space travel.

HZE particles make up approximately 1% of GCR, but are a significant contributor to dose in low-earth orbit because of their weight and high energy. Of all the particles in the spectrum, iron is thought to be the most important because of its relatively high-LET (*5*). A 1GeV iron particle has a LET of 146 keV/µm. In addition, an iron particle can produce significant delta rays as a result of its interaction with matter. Because of these characteristics of iron ions, its effect on biological systems is not completely understood, nor can it be directly extrapolated from alpha particles, electrons or x-rays. Research into understanding this effect was conducted by Burns *et al.*, and it was found that

electrons have a lower carcinogenic effectiveness than argon ions for skin tumor induction in rats (*16*). Moreover, the argon ion dose response seemed to follow a linear-quadratic response; however, the electron dose response was a dose cubed power function. Burns *et al.* hypothesize that this effect may result from the fact that the response to injury for each radiation type is by a different pathway. The different response pathways make it difficult to extrapolate dose response from a low-LET electron to a high-LET HZE particle; thus, experiments investigating the effects of HZE particles on biological tissue are necessary to understand all the repercussions of HZE exposure.

Therapeutic radiation exposure and accidental overexposures can result in the excess deposition of extracellular matrix components, or fibrosis. This wound response is often described as dead scar tissue (*78*); however, recently published research describes fibrosis differently. It has been determined that fibrosis is an active process which continuously reorganizes extracellular matrix components (*34*). Normally once a tissue repair response has been initiated, negative feedback mechanisms will conclude the repair response once the epithelium is fully regenerated. If this negative feedback is not initiated, or is somehow curtailed, then the tissue continually deposits and reorganizes the extracellular matrix; thus, resulting in fibrosis. Understanding the tissue response and why the interruption of the signal process results in fibrosis is necessary in order to treat or prevent a fibrotic response. There is still a great deal of research needed to complete this understanding; however, the initial activation of the repair response has

been determined to be caused by the activation of the cytokine, TGF-beta.

TGF-beta is known to have a significant role in a tissue's response to injury. This role is well defined for mechanical injury of tissue; however, it has just recently been investigated for its role in radiation-induced injury. Radiation-induced injury is sometimes considered a more dangerous type of injury because the stimulant is spread over a large area, but it has been shown that the tissue responds in a very similar pathway as it does to mechanical injury (*79*). Therefore, TGF-beta may also have just as significant a role in radiation-induced injury as in mechanical injury. In fact, research has shown that there is an over-response of TGF-beta in post-radiation treated cancer patients (*34, 80-82*). This excess response has been shown to cause fibrosis, which is a known precursor to carcinogenesis (*83, 84*). Bonniaud *et al.* have shown that if *Smad3*, the cytokine that is downstream in the signaling pathway of TGF-beta, is knocked out, there is no evidence of fibrosis or excess collagen accumulation.

TGF-beta is known to be activated in the response to radiation injury, and the interruption of its pathway downstream results in no fibrosis or collagen accumulation (*83*). Recent studies have also shown that irradiation of TFG-beta null mice had reduced downstream DNA damage (*85*) and null embryos fail to undergo apoptosis or inhibition of the cell cycle (*86*). These data show the importance of TGF-beta in the response to radiation, but the experiments focused on low-LET gamma-rays. Due to the different response of tissue to high and low-LET seen by Burns *et al.* the question of how the

TGF-beta pathway would respond to high-LET particles is left unanswered.

The movement of space travel to longer time and distances requires that future experiments address the variables astronauts would expect to see for such missions. The mixed field of high and low-LET radiation is a significant source of uncertainty, especially when trying to determine the fibrotic response in lung tissue. Recent experiments have shown that rat tissue responds differently to low and high-LET radiation and that TGF-beta activation is a precursor to fibrosis for low-LET irradiations; however, there is a lack of data addressing how TGF-beta will respond to high-LET radiation. The following experiments use the previously established perfusion chamber system as an *ex vivo* environment for determining if a change in TGF-beta response can be measured for high and low-LET irradiation. It is believed that by using a complete tissue model for measuring the response, a result that can be more closely related to what would be seen *in vivo* can be expected.

Materials and Methods

The materials and methods used for the housing of animals, harvesting tissue, and perfusion chamber preparation for the following experiments are as described in Chapter II.

Media

The media for the Brookhaven National Laboratory perfusion chamber trachea, BNL1, was prepared with two times the necessary growth factor components and later diluted

with Ham's F-12 for the normal concentration. BNL1, with two times the growth factors, consisted of the following components: Ham's F-12 (90.5%, Cambrex, Walkersville, MD), BSA-Factor V 7.5% (Gibco, Grand Island, NY), hEGF (0.004%, Cambrex, Walkersville, MD), gentamicin (0.2%, Cambrex, Walkersville, MD), hydrocortisone (0.02%, Cambrex, Walkersville, MD), insulin (0.1%, Cambrex, Walkersville, MD), transferrin (0.2%, Cambrex, Walkersville, MD), BPE (0.8%, Cambrex, Walkersville, MD).

Antibodies

Anti-TGF-beta antibody (R&D Systems, Minneapolis, MN) was used to pre-treat the perfusion chamber tracheas at 100 ng/mL concentration. This concentration corresponds to an approximate bioactivity neutralization of 95%. Samples were treated three hours prior to irradiation to insure sufficient time for the antibody to neutralize TGF-beta activity.

TGF-beta detection was completed using a rabbit polyclonal TGF-beta antibody (NIH, Kathy Flanders). After a sample were prepared and deparaffined, the slide was washed with cold Dulbecco's PBS (Gibco, Grand Island, NY) three times. The sample was then treated with a detergent wash (0.1% Trition X-100, Sigma, St. Louis, MO; 0.1% SSC, EM Science, Gibbstown, NJ) for two minutes and washed two times with PBS. The sample was blocked with 5% normal goat serum (Vector, Burlingame, CA) in DPBS for one hour at room temperature. LC-1-30-1 (S) rabbit anti-TGF-beta1 at 2 µg/mL in 5%

normal goat serum and DPBS was used to treat the sample for one hour at room temperature. After an hour, the sample was rinsed two times with DPBS and treated for 30 minutes with FITC-goat-anti-rabbit IgG (Zymed, San Francisco, CA) at a 1:200 concentration in 5% normal goat serum and DPBS. During this treatment the samples were kept in the dark to avoid bleaching of the fluorescein label. After fluorescein treatment, the sample was rinsed three times with DPBS and then distilled water. The sample was then blotted dry, treated with Vectashield (Vector, Burlingame, CA) and coverslipped. Finished samples were stored at 4° C.

Irradiations

X-ray irradiations were conducted at the Nuclear Science Center of Texas A&M University using a Norelco x-ray machine. All irradiations used 250 kVp x-rays. All HZE irradiations were conducted at Brookhaven National Laboratory's NASA Space Radiation Laboratory using 1Gev Fe particles.

Results

TGF-beta response after x-ray irradiation

Measurement of the TGF-beta antibody response for each x-ray treated tracheal section was made to determine if a response could be seen given the large auto fluorescence background intrinsic to tissue. Of the green spectrum, the signal used for analysis focused on bins 25 to 75 of 0 to 255 (white to bright green). It was determined that bins 25 to 75 provided the most fluorescence data directly correlating to a positive antibody

response and did not include bins which were saturated. In addition, analysis of this bin width proved there was no historical trend, or change in the treatment of the samples over time, in the fluorescence data. Once the correct bin width was determined, the negative antibody control, minus plus, was then subtracted from the positive control, plus plus, in order to see only the TGF-beta contribution to the signal. After subtracting the negative control from the positive TGF-beta signal, it was found that there was a discernable TGF-beta response (Fig. 17).

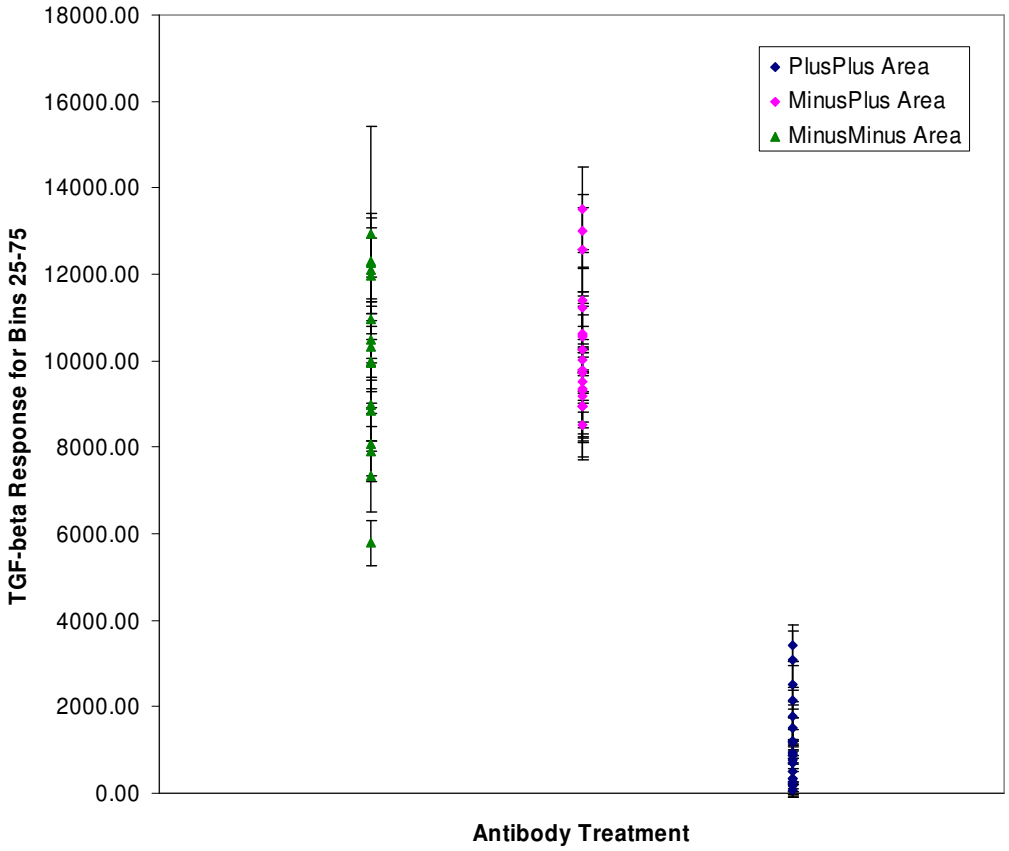

FIG. 17. The TGF-beta antibody response for 21 trachea irradiated with 250 kVp x-rays.

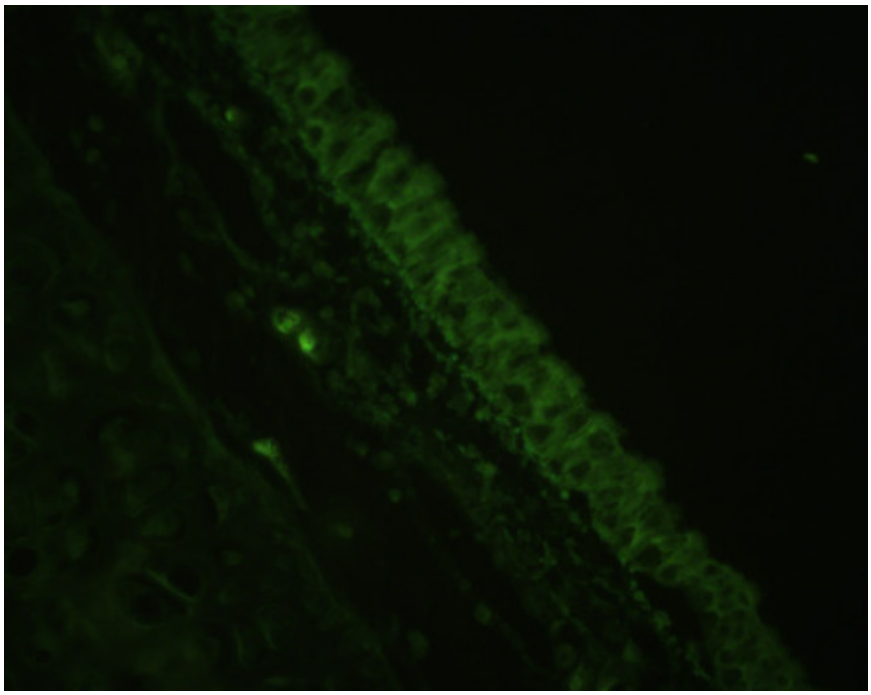

A

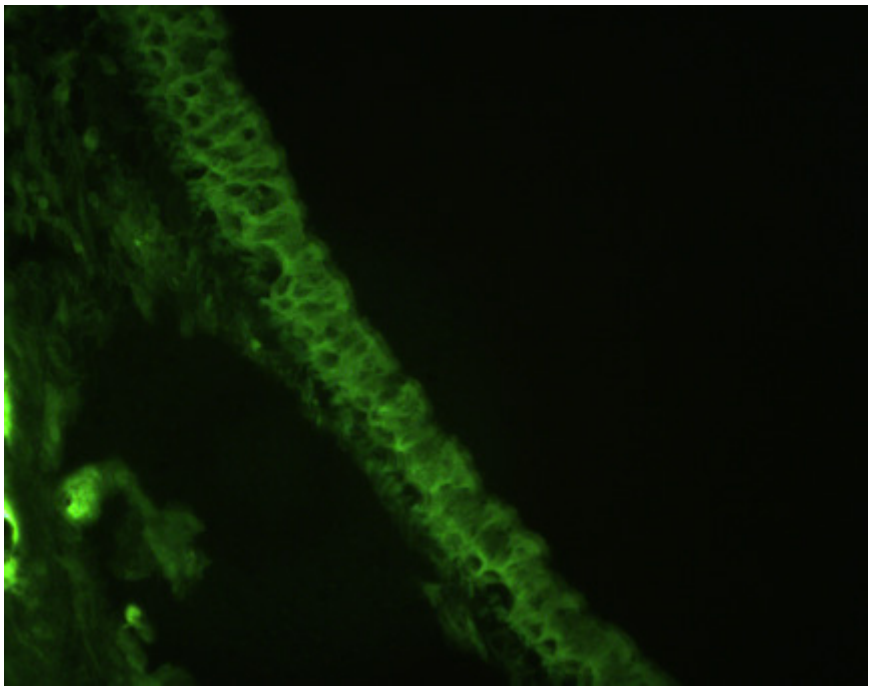

B

FIG. 18. Perfusion chamber trachea irradiated with 250 kVp x-rays at 2 cGy (A) and 100 cGy (B) and fixed at 0 hour. For this fixation time there seems to be an increased TGF-beta activation for increased dose.

The TGF-beta response after irradiation can be seen in x-ray irradiated tracheal tissue. The overall measured TGF-beta activation seems to be directly correlated for the 2 cGy and 100 cGy x-ray irradiated 0 hour fixed samples, or those samples fixed immediately after irradiation, and can be seen in the tracheal images (see Fig. 18).

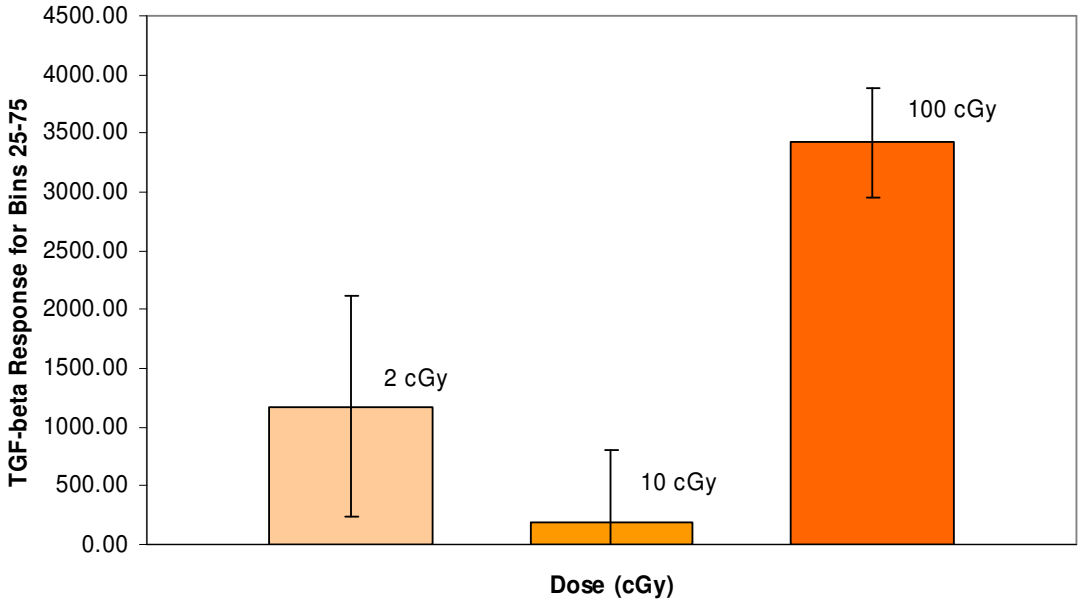

FIG. 19. The TGF-beta antibody response for x-ray irradiated trachea 0 hour post irradiation.

The 0 hour fixation, 10 cGy x-ray irradiation does not follow the same direct correlation found in the 2 cGy and 100 cGy doses (see Fig. 19). The reason for this is unclear, but the high error for the 10 cGy dose may indicate the sample signals are contaminated and obstructed by another variable. However, for the same x-ray dose and increased fixation times, 6 hour and 8 hour, the dose response is inversely related (images not shown).

Due to the lack of directly correlating doses and TGF-beta responses at each time point, a time course for the TGF-beta response for each dose was analyzed (see Fig. 20). It was found that there is a change in response time of the trachea based on the initial dose. For the highest dose, 100 cGy, the perfusion chamber trachea responded quickly to the irradiation and quickly decreased at six and eight hours. In contrast, the perfusion chamber trachea responded slowly to the 10 cGy irradiation, but had a marked increase at 8 hour post irradiation. Based on these data, the amount and speed of the tissue response is determined by the initial dose.

To determine if this response could be modulated, perfusion chambers were treated with a commercially available TGF-beta interfering antibody. A measured decrease of the TGF-beta response could be seen in the tracheal images of the TGF-beta interfering antibody treated perfusion chambers as compared to the untreated perfusion chamber tracheas (see Fig. 21). Moreover, a reduced TGF-beta response was seen in the blocked

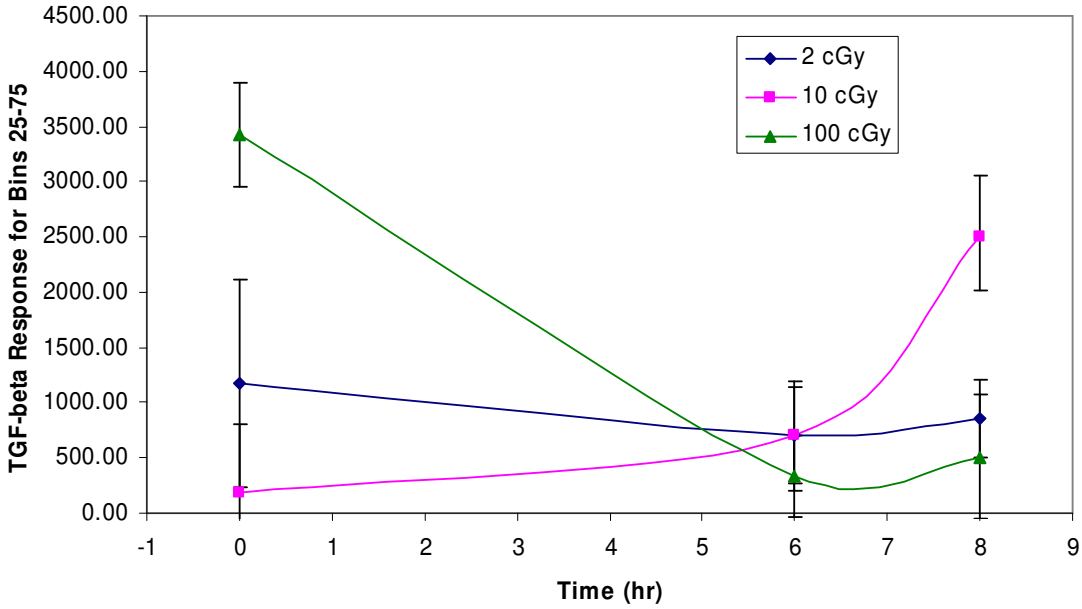

FIG. 20. The TGF-beta response over time of x-ray irradiated trachea at 2, 10 and 100 cGy.

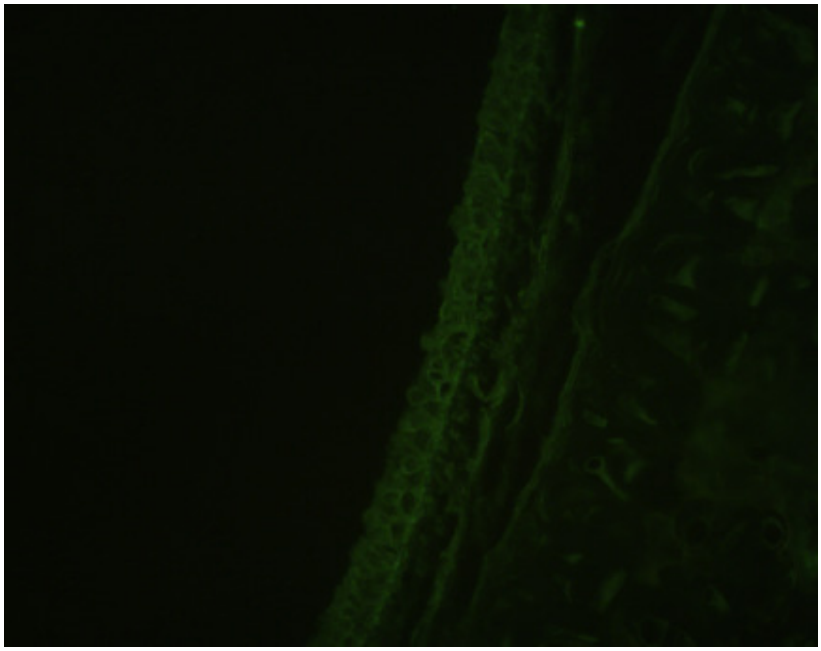

A

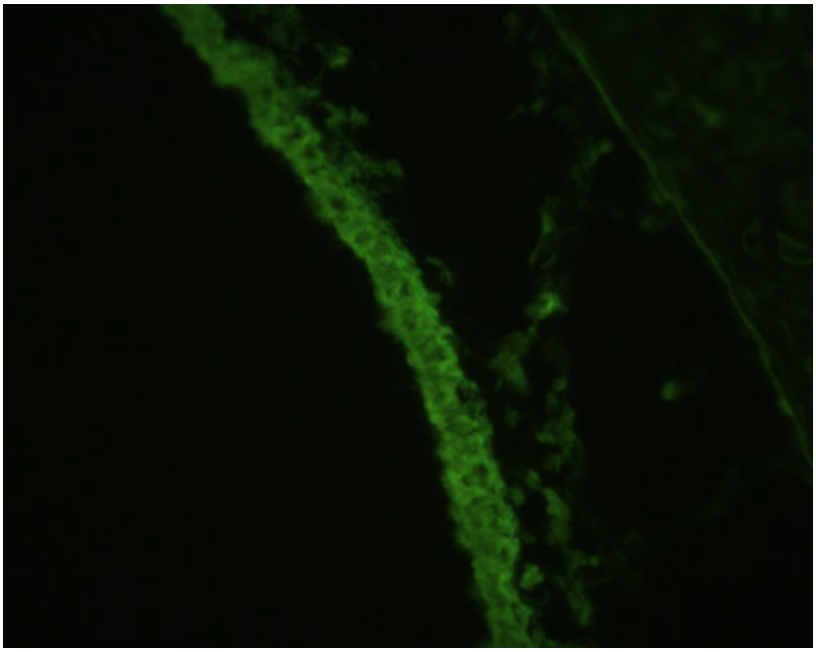

B

FIG. 21. TGF-beta interfering antibody treated (A) and untreated (B) trachea. Each trachea was irradiated with 100 cGy of x-rays and fixed at 0 hour. There is a reduction in the overall TGF-beta response in the epithelial layer in the treated trachea as compared to the untreated trachea.

TGF-beta perfusion chambers irradiated with x-rays (see Fig. 22). However, there was an increase in the TGF-beta signal at 6 hour and 8 hour post irradiation. This may indicate the interfering antibody was losing effectiveness or the cells were producing more TGF-beta. These data ensured that the TGF-beta blocking antibody was in fact blocking the TGF-beta activation during the perfusion chamber irradiations. Because a positive TGF-beta response was measured in x-ray treated perfusion chamber tracheas, further experiments were done to determine if a similar response could be found in HZE-treated tracheas.

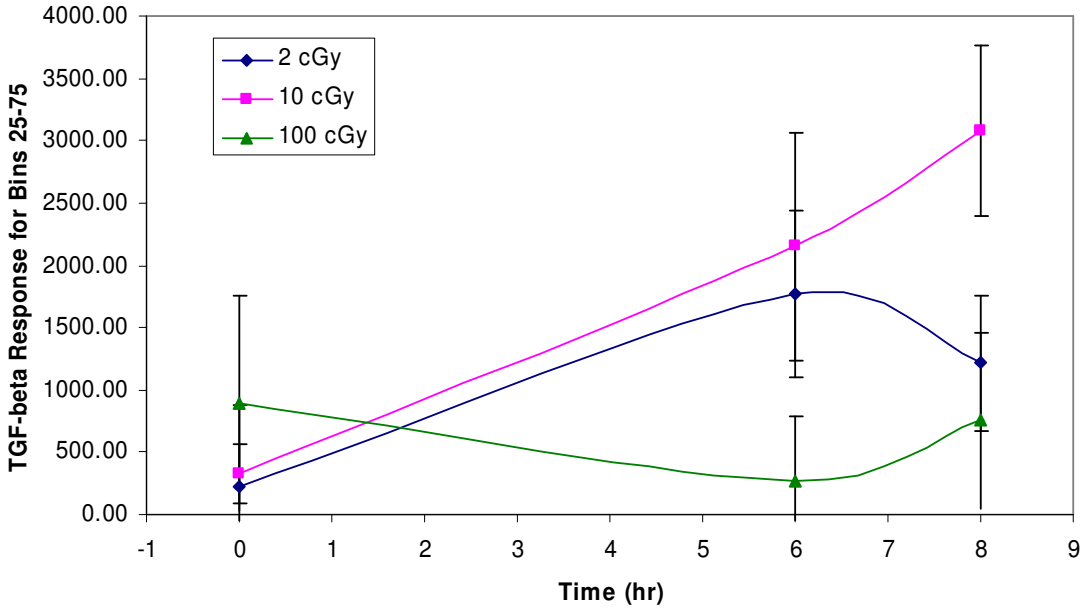

FIG. 22. The TGF-beta response over time of TGF-beta antibody interfered irradiated trachea at 2, 10 and 100 cGy.

Moreover, a reduced TGF-beta response was observed in the blocked TGF-beta perfusion chambers irradiated with x-rays (see Fig. 22). However, there was an increase in the TGF-beta signal at 6 hour and 8 hour post irradiation. This may indicate that the interfering antibody was losing effectiveness or the cells were producing more TGF-beta.

TGF-beta response after HZE irradiation

TGF-beta antibody experiments with Fe ion treated perfusion chamber tracheas were performed and the illumination measured using a light microscope. It can be seen in Fig. 23 that there was a significant difference between the negative controls and the positive TGF-beta signal (corrected for background). This response assured that the TGF-beta antibody signal could be measured for the x-ray and HZE treated trachea and used to determine if there was a change in the overall response of the tissue TGF-beta levels.

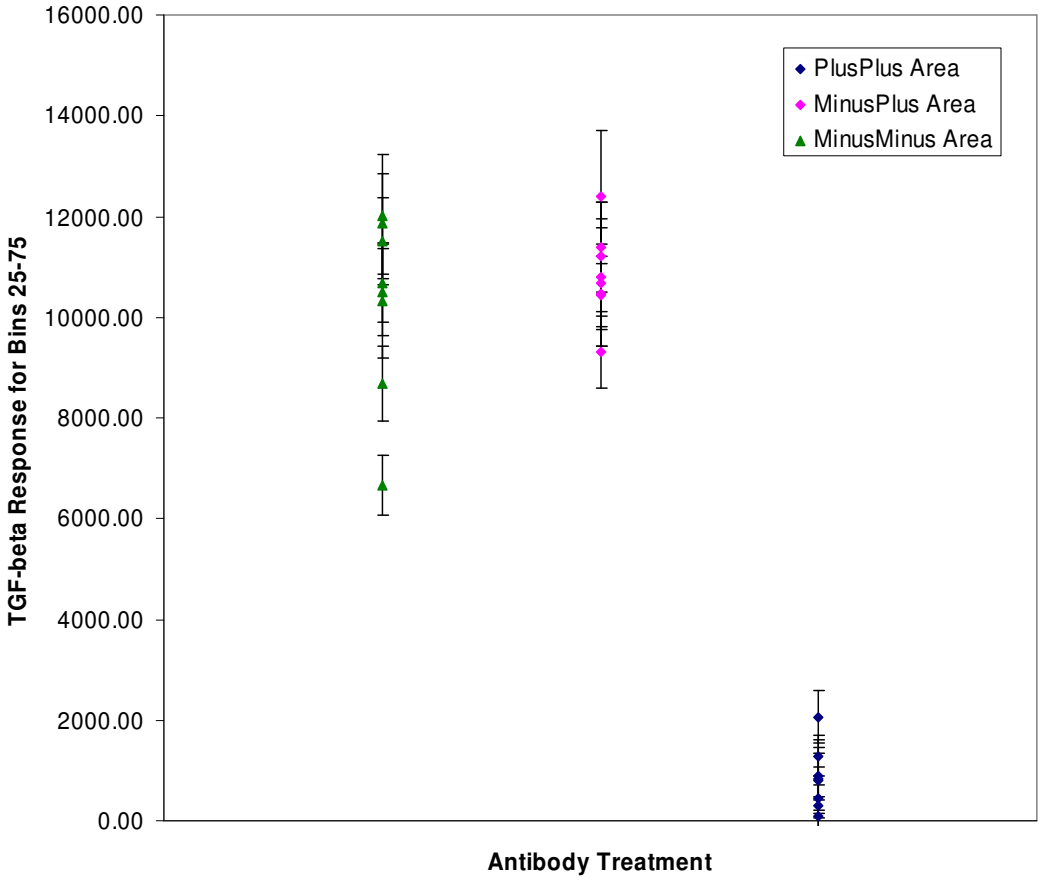

FIG. 23. The TGF-beta antibody response for eight trachea irradiated with 1 GeV Fe ions.

The dose response relationship for HZE irradiations was not as clear as for x-ray irradiations. Similar to the x-ray irradiations, it was found that the overall TGF-beta response was higher for a dose of 10 cGy than for 100 cGy at an 8 hour fixation time (see Fig. 24 and 25). Thus, indicating an inverse dose response for TGF-beta to HZE irradiations.

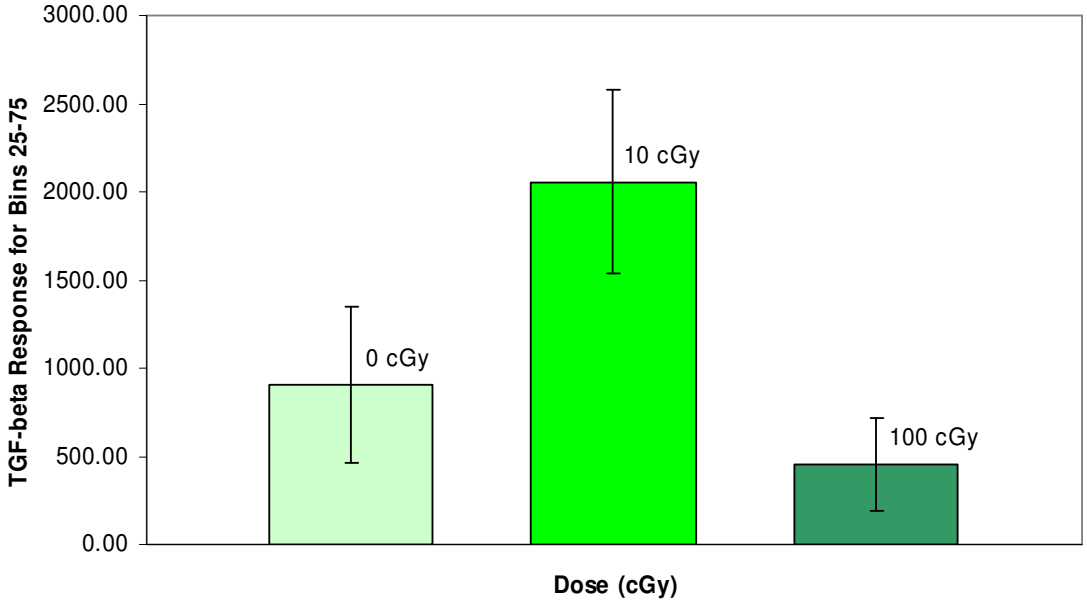

FIG. 24. The TGF-beta antibody response for HZE irradiated trachea 8 hour post irradiation.

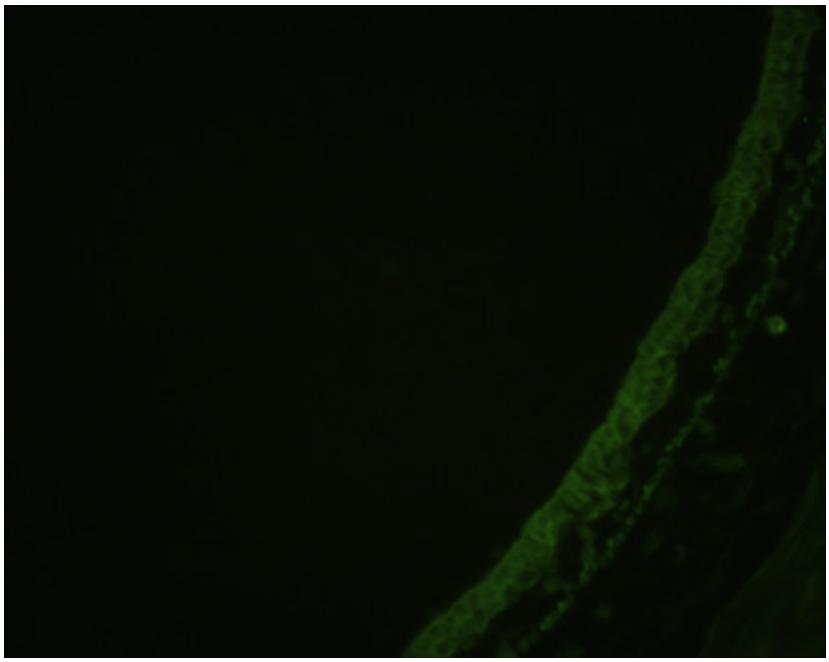

A

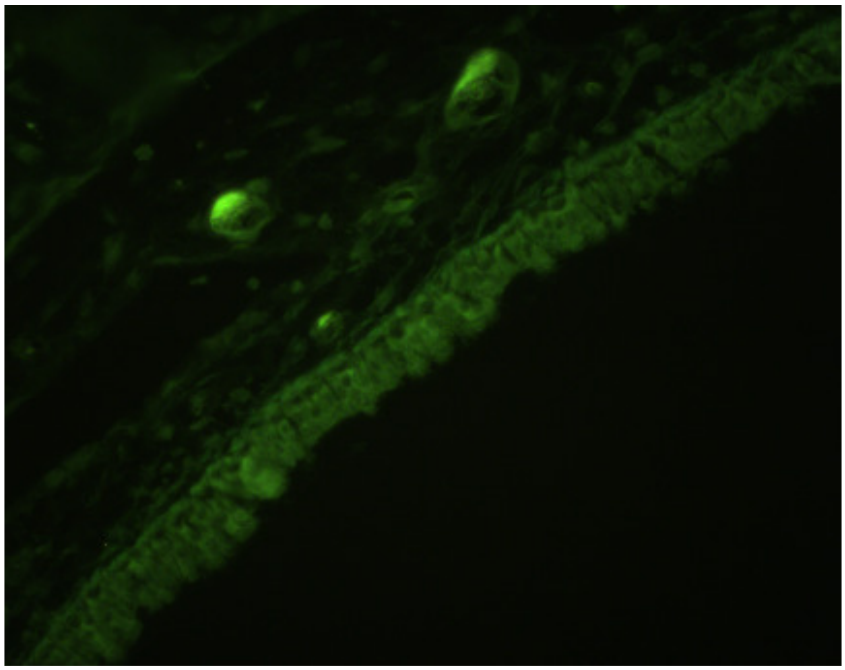

B

FIG. 25. Perfusion chamber trachea irradiated with 1 Gev Fe ions at 100 cGy (A) and 10 cGy (B) and fixed at 8 hour. For this fixation time there seems to be a decreased TGF-beta activation for increased dose.

However, the 0 cGy, HZE irradiated sample did not follow the same inverse dose relationship seen for 10 cGy and 100 cGy. Again, the reason for this is unclear but may be due to variables interfering with the sample fluorescence.

Comparison of HZE and x-ray TGF-beta response

After it was determined that the TGF-beta antibody could be used to measure the TGF-beta response after irradiation, a TGF-beta blocking antibody was used to attempt interruption of the downstream effects of TGF-beta. Measurements of the TGF-beta response after irradiation and TGF-beta blocking antibody treatment were taken to establish the efficacy of the blocking antibody. It was determined that a blocking TGF-beta antibody was effective at inhibiting TGF-beta response after irradiation (see Fig. 21).

Despite the efficacy of the TGF-beta interfering antibody, there was no clear differentiation between the x-ray irradiated trachea blocked for TGF-beta and those that were not or between the TGF-beta blocked x-ray and HZE irradiated tracheal tissue (see Fig. 26). Therefore, while the perfusion chamber system was able to provide data for overall TGF-beta response, it was not a model that could be used to measure the TGF-beta response after blocking the TGF-beta pathway using current methods.

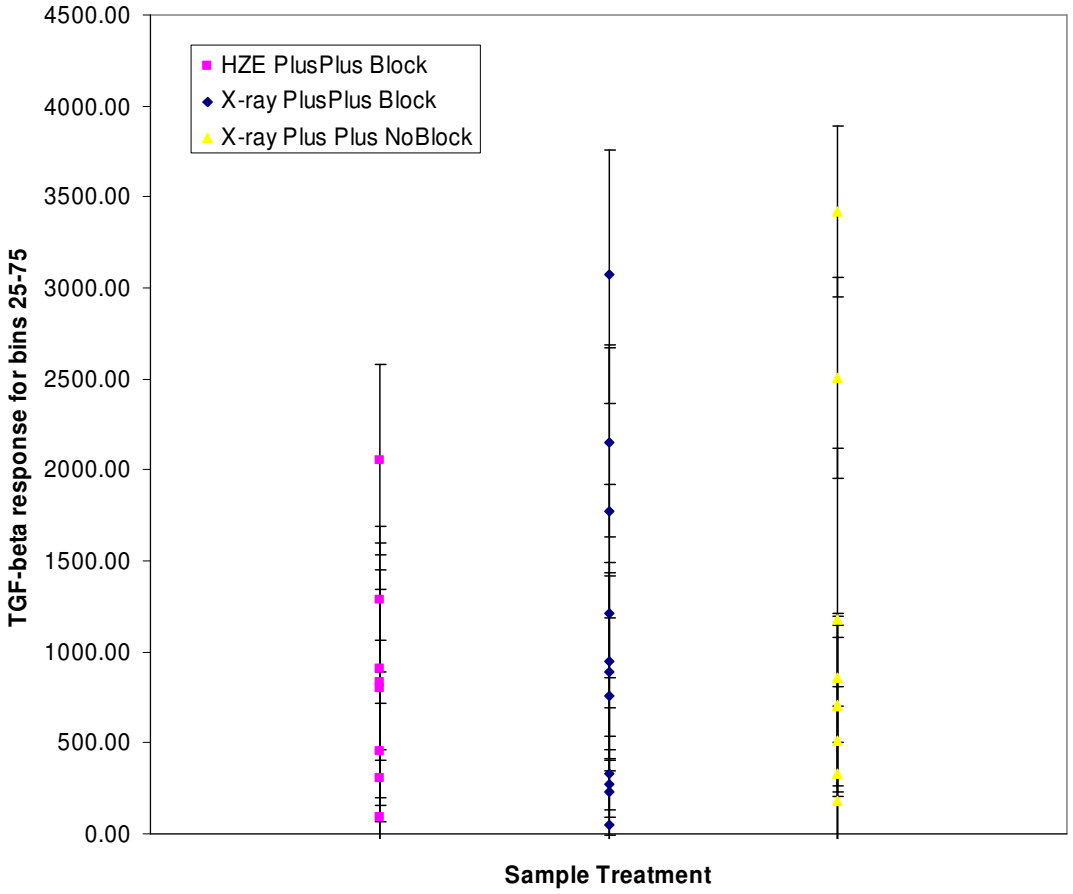

FIG. 26. The TGF-beta antibody response for 29 trachea irradiated with 250 kVp x-rays and 1 GeV Fe ions.

Discussion

Determination of the efficacy of the perfusion chamber as a model for the TGF-beta response in tissue was successfully demonstrated. After analysis of the overall TGF-beta response in x-ray and HZE treated samples, for all time points and doses, it was

determined that a significant difference could be found between the negative controls and the positive samples (corrected for background). Therefore, the perfusion chamber system was found to be a good model for measuring overall TGF-beta response of an *ex vivo* tracheal tissue sample.

In addition to ensuring that the overall TGF-beta result could be measured, it was necessary to interrupt the TGF-beta pathway to establish its effect on the tissue response to irradiation. A commercially available TGF-beta blocking antibody was used to block the pathway for both x-ray and HZE treated tissue samples. It is unclear from the data whether the blocking antibody was effective in blocking the active TGF-beta. Early indicators showed that for x-ray treated perfusion chamber trachea, the TGF-beta signal may be blocked at the 0 hour time point. The signal does not remain suppressed, and actually increases at the 6 hour and 8 hour time points. This could be due to a loss of effectiveness of the blocking antibody or the production of more active TGF-beta. One possibility is that the TGF-beta blocking antibody may not be able to penetrate sufficiently to attach and interfere with the active TGF-beta for long periods of time. Further investigation is needed to determine the increase in signal after the TGF-beta interference.

The benefit of working with a tissue model was the integration of variables not found in cell culture models. Multiple cell types, cartilage rings, increased cell-cell signaling, uncontrollable growth factors, etc. all play a role in the response of a tissue to stimuli. In

an effort to incorporate these into the experimental perfusion chamber model, one of these factors may have interrupted or compensated for the interrupted TGF-beta pathway. However, it was found that an overall TGF-beta response could be clearly measured using TGF-beta antibodies. The effectiveness of this measurement technique could be used to determine changes in the overall TGF-beta response for higher doses and multiple particle types. This TGF-beta measurement will not determine if there is an increased extracellular matrix deposition in the tissue, but it could show that a tissue TGF-beta response is different for higher doses and multiple particles.

CHAPTER V

CONCLUSIONS

Extended space travel poses a significant risk to the health of the mission team. Humans are well adapted to the terrestrial environment and are unprepared for the harsh conditions found in low earth orbit (LEO) and beyond. This environment consists of reduced gravity and a higher background of radiation as compared to the earth's surface; terrestrial organisms are protected by these conditions by earth's atmosphere and intrinsic magnetic fields. Despite this unique environment, much of the radiation research focuses on the gamma-ray effects on cellular models and does not address the effects of high-Z-high-energy (HZE) particles on a whole tissue.

The radiation dose an astronaut will be exposed to on long-term missions is thought to be one of the most limiting factors for missions. Because the mission is outside the earth's atmosphere and magnetic field, the team will be exposed to high-LET in addition to low-LET radiation. The two sources of high and low-LET radiation, galactic cosmic rays (GCR) and solar particle events (SPE), provide a different radiation spectrum but both contain HZE particles including: hydrogen, helium, carbon, neon, oxygen, silicon, and iron ions. Of these, the most significant contributor to the overall HZE dose is iron ions due to its high-LET of approximately 146 keV/μm. HZE particles are known to cause damage differently than low-LET radiation and affect the repair process of a cell. While low-LET radiation deposits energy in a random distribution through a medium,

HZE particles deposit most of their energy localized on the primary particle pathway. This localized energy deposition results in a dense ionization path. In addition, repair seems to be affected by high-LET radiation. The double-strand breaks (DSBs) caused by low-LET radiation are repaired at a higher average than those caused by high-LET radiation. Moreover, Goodwin and Blakely found that there is a decrease in the number of DSB repaired as the LET is increased (*14*). Thus, tissue response to radiation depends on the energy deposition pattern of the radiation.

Damage by radiation is also known to cause extracellular damage and may result in scarring or fibrosis of the wound area. The reconstruction of a damaged tissue follows a process that is independent of the type of injury (mechanical vs. radiation); however, the mechanical repair process tends to be localized as a result of local injury in contrast to widespread damage due to irradiation. In the case of an organism, this overall damage can cause organ failure or extensive damage in a specific organ (*79*). The repair of extracellular damage caused by radiation is known to be initiated by TGF-beta and, in the case of whole tissue, can result in tissue fibrosis and later cancer. The effects of TGF-beta activation post-irradiation, and its role in fibrosis, is well established with gamma-rays but has not been well studied with HZE particles.

Studies of the effects of HZE on biological systems and the contribution of a tissue to a cell's response to stimuli are moving forward. More researchers are publishing results on the effects of HZE and using whole tissue as a model for organism response to

radiation injury. However, there are currently no data on how a tracheal tissue responds to HZE radiation. The focus of this study was to determine if a discernable response could be measured in an *ex vivo* tissue model exposed to HZE particles. Based on this hypothesis a working *ex vivo* model for rat tracheal tissue was developed. In addition, it was shown that this model can be used for radiation experiments, including HZE. The TGF-beta response of the tissue to HZE and x-ray radiation did show a significant difference between the negative controls and the positive controls, despite the high auto fluorescent background intrinsic to tissue. The TGF-beta signal, however, did not indicate a significant difference between the radiation types.

Biological Aspects of Model Design

Cell culture models have been essential in the understanding of radiation effects. The research using these models has provided important data on intracellular pathways and bystander effects post irradiation. However, these models do not integrate the contributions to radiation effects by extracellular matrix components. Moreover, the cells in cellular *in vitro* models do not senesce. While this makes it easier to culture the cell line, immortal cells are rarely seen *in vivo* and are thought to be limited to stem cells. In an effort to mimic the *in vivo* environment, an *ex vivo* model for rat trachea was successfully developed.

Gabridge and Hoglund as well as Marcus and Baker were the first to develop a perfusion chamber system for guinea pig trachea. Their model was designed for studying bacterial

infection and was not adaptable for radiation experiments. A design, based on the original perfusion chamber, was developed using commercially available coverglass wells, to allow radiation experiments to be conducted without significant shielding (see Fig. 5).

After analysis of propidium iodide staining, physical damage to the epithelium, and PCNA antibody reaction, it was determined that the coverglass well perfusion chamber maintained the tracheal tissue in a healthy and viable condition for up to three days. Thus, irradiation experiments were performed within the first 24 hours and the trachea remained in the perfusion chamber less than 72 hours (see Fig. 10).

The successful development of a perfusion chamber system, adapted for irradiation experiments, allowed for the introduction of numerous *in vivo* variables: multiple cell types, cartilage rings, increased cell-cell signaling, growth factors, and nutritional needs. It is thought that these variables would cause a cell to respond more like an *in vivo* cell and provide a more direct correlation between *in vitro* and *in vivo* data (see Fig. 9 and Fig. 15).

Radiological Aspects of Model Design

Current radiation dose limits are based on the linear non-threshold extrapolation from high doses to zero. Underlying the linear extrapolation argument is the assumption that a cell responds autonomously to low doses of radiation. However, cells are stimulated to

divide, differentiate, or self destruct by neighboring cells and the extracellular matrix. In addition, there are data suggesting that unirradiated cells in an irradiated population may alter their level of repair related proteins (*65*) and their DNA metabolism (*22, 66, 67*). Therefore, it is very likely that an irradiated cell does not act autonomously but is influenced by its environment.

The gene expression of perfused rat trachea was examined to determine the effects of the perfusion chamber and radiation on the cells in the trachea. It was found that the gene expression of perfused trachea was not significantly different compared to fresh trachea. There was an increase in genes associated with mucus secretion, but this may be a result of the media, used to hydrate and provide nutrition for the cells, flowing through the lumen. In contrast, the 250 kVp x-ray irradiated trachea showed an eight-fold increase for CDKN1A expression. CDKN1A functions as a regulator of cell cycle progression at G1 and can interact with PCNA. Thus, the low dose of x-rays could be activating repair processes or arresting the cells.

The gene expression array further supported the perfusion chamber model as a design for mimicking *in vivo* trachea. However, further research into the effects of increased mucus production on the cell response to radiation needs to be investigated. The gene expression array also showed a measurable response was found post low-doses of low-LET radiation. This measurement technique could be used in the future to better understand the response of a whole tissue to radiation in an *ex vivo* environment.

Comparative Effects of Low- and High-LET

TGF-beta is an important signal transducer and is activated in response to injury. Active TGF-beta is known to have three major roles in tissue: immunosuppression, deposition of extracellular matrix components, and cell growth inhibition. The continual deposition of extracellular matrix components due to the activation of TGF-beta is a significant part of fibrosis of tissue. This response has been proven in irradiated tissue and can be stopped or reduced by inactivating TGF-beta. However, low-LET radiation is the only radiation type used to study TGF-beta activation. A large gap in the published data exists for the TGF-beta response to high-LET radiation after TGF-beta inactivation.

This research studied the effect of high-LET Fe ions on the overall TGF-beta response after TGF-beta inactivation and compared the results to the TGF-beta response post x-ray irradiation. It was found that a TGF-beta response could be measured in the tracheal tissue, for x-ray and Fe ion irradiations, despite the high autofluorescent background intrinsic to tissue. However, after comparing the TGF-beta response of x-ray irradiation to HZE irradiation, there was not a significant difference in radiation types. Clearly, this may be because the tissue TGF-beta responses to low doses of low- and high-LET radiation are similar, thus indicating the published fibrosis data using low-LET radiation describes the response that would be seen for high-LET. However, the TGF-beta response could be masked by interfering signals intrinsic to a tissue with multiple cell types and increased cell signaling.

The TGF-beta response in x-ray and HZE irradiated perfusion chambers was also measured over time post irradiation. It was found that for 6 hour and 8 hour post irradiation, the TGF-beta response was higher for lower doses of radiation than for higher doses. This is in contrast to the 0 hour fixation which found the TGF-beta response to increase with increased dose. The inverse relationship found for 6 hour and 8 hour fixation times may indicate a threshold response for TGF-beta response; i.e., for low doses, a threshold of dose must be reached for an immediate TGF-beta response, or else the tissue responds more slowly to the irradiation damage. These data may also indicated that the speed of cell response to radiation is determined by the initial dose. This result was unexpected and will require further investigation to determine if the threshold or speed of response can be determined for the 250 kVp x-rays and 1 Gev Fe ions.

Future Work

The work completed in this project established the perfusion chamber system as an *ex vivo* model for studying radiation effects in respiratory tissue. It was determined that a measured difference in TGF-beta response could be detected between negative and positive controls. However, the TGF-beta response could not be differentiated between x-ray and HZE experiments, and the inability to measure a difference may be due to insensitivity of the immunohistochemistry technique. Therefore, to insure that the lack of difference between the two radiation types is not more than the limits of the measurement technique, more gene expression arrays should be completed. This would

support the results found in this research (or show the limits of the measurement techniques). In addition, more TGF-beta response experiments should be completed to determine if a threshold can be determined for its response. The preliminary results indicate that a threshold may exist and gene expression arrays could help to clearly elucidate a threshold.

The repopulation experiments attempted in this project were not a success; however, repopulation of xenografts has proven successful. Xenografts are a step closer to *in vivo* but are limited in the number of variables (radiation type, nutrition, etc.) that can be introduced into the experiment. It is believed that perfusion chamber trachea repopulated with human cells would provide excellent data to link human, animal, and cell research, and as more experiments into repopulating trachea as new techniques become available the research in this are should move forward.

The establishment of an *ex vivo* model for radiation experiments with respiratory tissue opens the door for more research into correlating data between cell culture models and *in vivo* data. While the perfusion chamber is not a perfect model for *in vivo*, it allows for more intricate experiments using intact tissue, including: microbeam irradiations using cell culture and perfusion chamber models. The data would further support the previous work studying bystander effects and their role in creating a preneoplastic condition.

REFERENCES

1. S. M. Smith and M. Heer, Calcium and bone metabolism during space flight. *Nutrition* **18**, 849-852 (2002).

2. M. A. Bender, P. C. Gooch and S. Kondo, The Gemini-3 S-4 spaceflight-radiation interaction experiment. *Radiat Res* **31**, 91-111 (1967).

3. M. A. Bender, P. C. Gooch and S. Kondo, The Gemini XI S-4 spaceflight-radiation interaction experiment: the human blood experiment. *Radiat Res* **34**, 228-238 (1968).

4. J. Kiefer and H. D. Pross, Space radiation effects and microgravity. *Mutat Res* **430**, 299-305 (1999).

5. National Council on Radiation Protection and Measurements., *Radiation Protection Guidance for Activities in Low-Earth Orbit : Recommendations of the Nattional Council on Radiation Protection and Measurements*. National Council on Radiation Protection and Measurements, Bethesda, Md., 2000.

6. N. Desai, E. Davis, P. O'Neill, M. Durante, F. A. Cucinotta and H. Wu, Immunofluorescence detection of clustered gamma-H2AX foci induced by HZE-particle radiation. *Radiat Res* **164**, 518-522 (2005).

7. E. A. Blakely and A. Kronenberg, Heavy-ion radiobiology: new approaches to delineate mechanisms underlying enhanced biological effectiveness. *Radiat Res* **150**, S126-145 (1998).

8. M. Gulston, C. de Lara, T. Jenner, E. Davis and P. O'Neill, Processing of clustered DNA damage generates additional double-strand breaks in mammalian cells post-irradiation. *Nucleic Acids Res* **32**, 1602-1609 (2004).

9. B. Rydberg, B. Cooper, P. K. Cooper, W. R. Holley and A. Chatterjee, Dose-dependent misrejoining of radiation-induced DNA double-strand breaks in human fibroblasts: experimental and theoretical study for high- and low-LET radiation. *Radiat Res* **163**, 526-534 (2005).

10. B. M. Sutherland, P. V. Bennett, O. Sidorkina and J. Laval, Clustered DNA damages induced in isolated DNA and in human cells by low doses of ionizing radiation. *Proc Natl Acad Sci USA* **97**, 103-108 (2000).

11. J. Heilmann, H. Rink, G. Taucher-Scholz and G. Kraft, DNA strand break induction and rejoining and cellular recovery in mammalian cells after heavy-ion irradiation. *Radiat Res* **135**, 46-55 (1993).

12. G. Kampf and K. Eichhorn, DNA strand breakage by different radiation qualities and relations to cell killing: further results after the influence of alpha-particles and carbon ions. *Stud. Biophys.* **93**, 17-26 (1983).

13. K. M. Prise, S. Davies and B. D. Michael, The relationship between radiation-induced DNA double-strand breaks and cell kill in hamster V79 fibroblasts irradiated with 250 kVp X-rays, 2.3 MeV neutrons or 238Pu alpha-particles. *Int J Radiat Biol Relat Stud Phys Chem Med* **52**, 893-902 (1987).

14. E. H. Goodwin and E. A. Blakely, Heavy ion-induced chromosomal damage and repair. *Adv Space Res* **12**, 81-89 (1992).

15. E. L. Alpen, P. Powers-Risius, S. B. Curtis and R. DeGuzman, Tumorigenic potential of high-Z, high-LET charged-particle radiations. *Radiat Res* **136**, 382-391 (1993).

16. F. J. Burns, Y. Jin, K. L. Koenig and S. Hosselet, The low carcinogenicity of electron radiation relative to argon ions in rat skin. *Radiat Res* **135**, 178-188 (1993).

17. J. F. Dicello, A. Christian, F. A. Cucinotta, D. S. Gridley, R. Kathirithamby, J. Mann, A. R. Markham, M. F. Moyers, G. R. Novak, et al., In vivo mammary tumourigenesis in the Sprague-Dawley rat and microdosimetric correlates. *Phys Med Biol* **49**, 3817-3830 (2004).

18. C. Mothersill and C. Seymour, Radiation-induced bystander effects: past history and future directions. *Radiat Res* **155**, 759-767 (2001).

19. M. H. Barcellos-Hoff and A. L. Brooks, Extracellular signaling through the microenvironment: a hypothesis relating carcinogenesis, bystander effects, and genomic instability. *Radiat Res* **156**, 618-627 (2001).

20. W. F. Morgan, Non-targeted and delayed effects of exposure to ionizing radiation: II. Radiation-induced genomic instability and bystander effects in vivo, clastogenic factors and transgenerational effects. *Radiat Res* **159**, 581-596 (2003).

21. W. F. Morgan, Non-targeted and delayed effects of exposure to ionizing radiation: I. Radiation-induced genomic instability and bystander effects in vitro. *Radiat Res* **159**, 567-580 (2003).

22. H. Nagasawa and J. B. Little, Induction of sister chromatid exchanges by extremely low doses of alpha-particles. *Cancer Res* **52**, 6394-6396 (1992).

23. H. Nagasawa and J. B. Little, Unexpected sensitivity to the induction of mutations by very low doses of alpha-particle radiation: evidence for a bystander effect. *Radiat Res* **152**, 552-557 (1999).

24. K. M. Prise, O. V. Belyakov, M. Folkard and B. D. Michael, Studies of bystander effects in human fibroblasts using a charged particle microbeam. *Int J Radiat Biol* **74**, 793-798 (1998).

25. C. P. Yu and G. B. Xu, Predictive models for deposition of inhaled diesel exhaust particles in humans and laboratory species. *Res Rep Health Eff Inst*, 3-22 (1987).

26. Y. Inayama, G. E. Hook, A. R. Brody, A. M. Jetten, T. Gray, J. Mahler and P. Nettesheim, In vitro and in vivo growth and differentiation of clones of tracheal basal cells. *Am J Pathol* **134**, 539-549 (1989).

27. J. E. Boers, J. L. den Brok, J. Koudstaal, J. W. Arends and F. B. Thunnissen, Number and proliferation of neuroendocrine cells in normal human airway epithelium. *Am J Respir Crit Care Med* **154**, 758-763 (1996).

28. P. Demoly, J. Simony-Lafontaine, P. Chanez, J. L. Pujol, N. Lequeux, F. B. Michel and J. Bousquet, Cell proliferation in the bronchial mucosa of asthmatics and chronic bronchitics. *Am J Respir Crit Care Med* **150**, 214-217 (1994).

29. N. F. Johnson and A. F. Hubbs, Epithelial progenitor cells in the rat trachea. *Am J Respir Cell Mol Biol* **3**, 579-585 (1990).

30. M. H. Barcellos-Hoff, C. Park and E. G. Wright, Radiation and the microenvironment - tumorigenesis and therapy. *Nat Rev Cancer* **5**, 867-875 (2005).

31. D. A. Lawrence, Latent-TGF-beta: an overview. *Mol Cell Biochem* **219**, 163-170 (2001).

32. R. A. Ignotz and J. Massague, Transforming growth factor-beta stimulates the expression of fibronectin and collagen and their incorporation into the extracellular matrix. *J Biol Chem* **261**, 4337-4345 (1986).

33. A. Leask and D. J. Abraham, TGF-beta signaling and the fibrotic response. *Faseb J* **18**, 816-827 (2004).

34. M. Martin, J. Lefaix and S. Delanian, TGF-beta1 and radiation fibrosis: a master switch and a specific therapeutic target? *Int J Radiat Oncol Biol Phys* **47**, 277-290 (2000).

35. C. C. Park, M. J. Bissell and M. H. Barcellos-Hoff, The influence of the microenvironment on the malignant phenotype. *Mol Med Today* **6**, 324-329 (2000).

36. E. S. Yi, A. Bedoya, H. Lee, E. Chin, W. Saunders, S. J. Kim, D. Danielpour, D. G. Remick, S. Yin and T. R. Ulich, Radiation-induced lung injury in vivo: expression of transforming growth factor-beta precedes fibrosis. *Inflammation* **20**, 339-352 (1996).

37. M. Kolb, P. J. Margetts, P. J. Sime and J. Gauldie, Proteoglycans decorin and biglycan differentially modulate TGF-beta-mediated fibrotic responses in the lung. *Am J Physiol Lung Cell Mol Physiol* **280**, L1327-1334 (2001).

38. O. Sanli, A. Armagan, E. Kandirali, B. Ozerman, I. Ahmedov, S. Solakoglu, A. Nurten, M. Tunc, V. Uysal and A. Kadioglu, TGF-beta1 neutralizing antibodies decrease the fibrotic effects of ischemic priapism. *Int J Impot Res* **16**, 492-497 (2004).

39. E. J. Ehrhart, P. Segarini, M. L. Tsang, A. G. Carroll and M. H. Barcellos-Hoff, Latent transforming growth factor beta1 activation in situ: quantitative and functional evidence after low-dose gamma-irradiation. *Faseb J* **11**, 991-1002 (1997).

40. S. Xavier, E. Piek, M. Fujii, D. Javelaud, A. Mauviel, K. C. Flanders, A. M. Samuni, A. Felici, M. Reiss, et al., Amelioration of radiation-induced fibrosis: inhibition of transforming growth factor-beta signaling by halofuginone. *J Biol Chem* **279**, 15167-15176 (2004).

41. A. F. Hubbs, F. F. Hahn and D. G. Thomassen, Increased resistance to transforming growth factor beta accompanies neoplastic progression of rat tracheal epithelial cells. *Carcinogenesis* **10**, 1599-1605 (1989).

42. M. Terzaghi-Howe, Changes in response to, and production of, transforming growth factor type beta during neoplastic progression in cultured rat tracheal epithelial cells. *Carcinogenesis* **10**, 973-980 (1989).

43. R. Iyer and B. E. Lehnert, Effects of ionizing radiation in targeted and nontargeted cells. *Arch Biochem Biophys* **376**, 14-25 (2000).

44. M. J. Bissell and M. H. Barcellos-Hoff, The influence of extracellular matrix on gene expression: is structure the message? *J Cell Sci Suppl* **8**, 327-343 (1987).

45. M. J. Whitcutt, K. B. Adler and R. Wu, A biphasic chamber system for maintaining polarity of differentiation of cultured respiratory tract epithelial cells. *In Vitro Cell Dev Biol* **24**, 420-428 (1988).

46. Y. You, E. J. Richer, T. Huang and S. L. Brody, Growth and differentiation of mouse tracheal epithelial cells: selection of a proliferative population. *Am J Physiol Lung Cell Mol Physiol* **283**, L1315-1321 (2002).

47. A. M. Collier, L. P. Peterson and J. B. Baseman, Pathogenesis of infection with Bordetella pertussis in hamster tracheal organ culture. *J Infect Dis* **136 Suppl**, S196-203 (1977).

48. B. Mintz and K. Illmensee, Normal genetically mosaic mice produced from malignant teratocarcinoma cells. *Proc Natl Acad Sci USA* **72**, 3585-3589 (1975).

49. J. Aggeler, J. Ward, L. M. Blackie, M. H. Barcellos-Hoff, C. H. Streuli and M. J. Bissell, Cytodifferentiation of mouse mammary epithelial cells cultured on a reconstituted basement membrane reveals striking similarities to development in vivo. *J Cell Sci* **99 (Pt 2)**, 407-417 (1991).

50. M. H. Barcellos-Hoff, J. Aggeler, T. G. Ram and M. J. Bissell, Functional differentiation and alveolar morphogenesis of primary mammary cultures on reconstituted basement membrane. *Development* **105**, 223-235 (1989).

51. K. L. Schmeichel and M. J. Bissell, Modeling tissue-specific signaling and organ function in three dimensions. *J Cell Sci* **116**, 2377-2388 (2003).

52. M. H. Barcellos-Hoff and S. A. Ravani, Irradiated mammary gland stroma promotes the expression of tumorigenic potential by unirradiated epithelial cells. *Cancer Res* **60**, 1254-1260 (2000).

53. E. J. Ehrhart, E. L. Gillette and M. H. Barcellos-Hoff, Immunohistochemical evidence of rapid extracellular matrix remodeling after iron-particle irradiation of mouse mammary gland. *Radiat Res* **145**, 157-162 (1996).

54. H. P. Rodemann and M. Bamberg, Cellular basis of radiation-induced fibrosis. *Radiother Oncol* **35**, 83-90 (1995).

55. M. G. Gabridge and L. E. Hoglund, Mycoplasma pneumoniae infection of intact guinea pig tracheas cultured in a unique matrix-embed/perfusion system. *In Vitro* **17**, 847-858 (1981).

56. H. Marcus and N. R. Baker, Quantitation of adherence of mucoid and nonmucoid Pseudomonas aeruginosa to hamster tracheal epithelium. *Infect Immun* **47**, 723-729 (1985).

57. A. J. Klein-Szanto, B. C. Pal, M. Terzaghi and A. C. Marchok, Heterotopic tracheal transplants: techniques and applications. *Environ Health Perspect* **56**, 75-86 (1984).

58. M. Terzaghi, P. Nettesheim and M. L. Williams, Repopulation of denuded tracheal grafts with normal, preneoplastic, and neoplastic epithelial cell populations. *Cancer Res* **38**, 4546-4553 (1978).

59. F. Dupuit, D. Gaillard, J. Hinnrasky, E. Mongodin, S. de Bentzmann, E. Copreni and E. Puchelle, Differentiated and functional human airway epithelium regeneration in tracheal xenografts. *Am J Physiol Lung Cell Mol Physiol* **278**, L165-176 (2000).

60. E. Puchelle and B. Peault, Human airway xenograft models of epithelial cell regeneration. *Respir Res* **1**, 125-128 (2000).

61. S. Escotte, C. Catusse, C. Coraux and E. Puchelle, Reconstitution of human airway tissue in the humanized xenograft model. *J Cyst Fibros* **3 Suppl 2**, 63-65 (2004).

62. J. R. Ford, A. J. Maslowski, R. A. Redd and L. A. Braby, Radiation responses of perfused tracheal tissue. *Radiat Res* **164**, 487-492 (2005).

63. G. Maga and U. Hubscher, Proliferating cell nuclear antigen (PCNA): a dancer with many partners. *J Cell Sci* **116**, 3051-3060 (2003).

64. J. M. Nelson, A. L. Brooks, N. F. Metting, M. A. Khan, R. L. Buschbom, A. Duncan, R. Miick and L. A. Braby, Clastogenic effects of defined numbers of 3.2 MeV alpha particles on individual CHO-K1 cells. *Radiat Res* **145**, 568-574 (1996).

65. A. S. Balajee and C. R. Geard, Chromatin-bound PCNA complex formation triggered by DNA damage occurs independent of the ATM gene product in human cells. *Nucleic Acids Res* **29**, 1341-1351 (2001).

66. A. Deshpande, E. H. Goodwin, S. M. Bailey, B. L. Marrone and B. E. Lehnert, Alpha-particle-induced sister chromatid exchange in normal human lung fibroblasts: evidence for an extranuclear target. *Radiat Res* **145**, 260-267 (1996).

67. H. Nagasawa, J. B. Little, W. C. Inkret, S. Carpenter, K. Thompson, M. R. Raju, D. J. Chen and G. F. Strniste, Cytogenetic effects of extremely low doses of plutonium-238 alpha-particle irradiation in CHO K-1 cells. *Mutat Res* **244**, 233-238 (1990).

68. P. V. Bhat, T. Bader, P. Nettesheim and A. M. Jetten, Differentiation-dependent regulation of retinal dehydrogenase gene expression in the trachea. *Biochem Cell Biol* **76**, 59-62 (1998).

69. M. Terzaghi-Howe, Induction of preneoplastic alterations by X rays and neutrons in exposed rat tracheas and isolated tracheal epithelial cells. *Radiat Res* **120**, 352-363 (1989).

70. M. Terzaghi-Howe, J. R. Ford and J. E. Turner, Influence of cell position relative to planar alpha-particle sources on survival and preneoplastic transformation of primary rat tracheal epithelial cells. *Radiat Res* **145**, 432-441 (1996).

71. M. Terzaghi-Howe, G. W. Chang and D. Popp, Emergence of undifferentiated rat tracheal cell carcinomas, but not squamous cell carcinomas, is associated with a loss of expression of E-cadherin and of gap junction communication. *Carcinogenesis* **18**, 2043-2050 (1997).

72. E. I. Azzam, S. M. de Toledo, T. Gooding and J. B. Little, Intercellular communication is involved in the bystander regulation of gene expression in human cells exposed to very low fluences of alpha particles. *Radiat Res* **150**, 497-504 (1998).

73. M. Terzaghi-Howe and C. McKeown, Inhibition of carcinogen-altered rat tracheal epithelial cells by normal epithelial cell-conditioned medium. *Cancer Res* **46**, 917-921 (1986).

74. J. R. Ford and M. Terzaghi-Howe, Effects of 210Po alpha particles on survival and preneoplastic transformation of primary rat tracheal epithelial cells irradiated while in suspension or in the intact tissue. *Radiat Res* **136**, 89-96 (1993).

75. S. A. Amundson, M. Bittner and A. J. Fornace, Jr., Functional genomics as a window on radiation stress signaling. *Oncogene* **22**, 5828-5833 (2003).

76. J. R. Ford and M. Terzaghi-Howe, Basal cells are the progenitors of primary tracheal epithelial cell cultures. *Exp Cell Res* **198**, 69-77 (1992).

77. M. Terzaghi-Howe and J. Ford, Effects of radiation on rat respiratory epithelial cells: critical target cell populations and the importance of cell-cell interactions. *Adv Space Res* **14**, 565-572 (1994).

78. S. R. Beanes, C. Dang, C. Soo and K. Ting, Skin repair and scar formation: the central role of TGF. *Expert Rev Mol Med* **2003**, 1-22 (2003).

79. M. H. Barcellos-Hoff, How tissues respond to damage at the cellular level: orchestration by transforming growth factor-{beta} (TGF-{beta}). *BJR Suppl* **27**, 123-127 (2005).

80. M. H. Barcellos-Hoff, R. Derynck, M. L. Tsang and J. A. Weatherbee, Transforming growth factor-beta activation in irradiated murine mammary gland. *J Clin Invest* **93**, 892-899 (1994).

81. R. P. Abratt and G. W. Morgan, Lung toxicity following chest irradiation in patients with lung cancer. *Lung Cancer* **35**, 103-109 (2002).

82. G. W. Morgan and S. N. Breit, Radiation and the lung: a reevaluation of the mechanisms mediating pulmonary injury. *Int J Radiat Oncol Biol Phys* **31**, 361-369 (1995).

83. P. Bonniaud, P. J. Margetts, K. Ask, K. Flanders, J. Gauldie and M. Kolb, TGF-beta and Smad3 signaling link inflammation to chronic fibrogenesis. *J Immunol* **175**, 5390-5395 (2005).

84. P. J. Sime, R. A. Marr, D. Gauldie, Z. Xing, B. R. Hewlett, F. L. Graham and J. Gauldie, Transfer of tumor necrosis factor-alpha to rat lung induces severe pulmonary inflammation and patchy interstitial fibrogenesis with induction of transforming growth factor-beta1 and myofibroblasts. *Am J Pathol* **153**, 825-832 (1998).

85. J. Kirshner, M. F. Jobling, M. J. Pajares, S. A. Ravani, A. B. Glick, M. J. Lavin, S. Koslov, Y. Shiloh and M. H. Barcellos-Hoff, Inhibition of transforming growth factor-beta1 signaling attenuates ataxia telangiectasia mutated activity in response to genotoxic stress. *Cancer Res* **66**, 10861-10869 (2006).

86. K. B. Ewan, R. L. Henshall-Powell, S. A. Ravani, M. J. Pajares, C. Arteaga, R. Warters, R. J. Akhurst and M. H. Barcellos-Hoff, Transforming growth factor-beta1 mediates cellular response to DNA damage in situ. *Cancer Res* **62**, 5627-5631 (2002).

APPENDIX A

PERFUSION CHAMBER PROTOCOLS

1. Anaesthetize rats 6 hours prior to irradiation.
2. Excise tracheas, hold on ice in separate 15 ml. tubes with 5 ml. of cold BNL1 (60 ml.).
3. For the next steps each trachea is treated separately through the entire procedure:
    a. Melt 3% sterile agarose in distilled water (enzyme free, Invitrogen)in 60C bath.
    b. Warm 2X BNL1 to 37C.
    c. Mix 6 ml. of agarose with 6 ml. of 2X BNL1 and lay down thin layer (2 ml.) in each chamber. Refrigerate briefly to set the gel.
    d. Dissect trachea to remove excess tissue and to yield 2 sections of roughly equal length. Retain excess pieces for histology.
    e. Mix 3 ml. of agarose with 3 ml. of 2X BNL1 (6 ml.).
    f. Place each section between two coverslips and pour an agarose overlayer. Refrigerate briefly to set the gel.
    g. Remove coverslips and clear lumen of any agarose using 1000 micropipettor and sterile tip with medium.
    h. Remove excess agarose.
    i. Fill chamber with 2-3 ml. of 1X BNL1 and place in incubator on rocking platform.
4. Repeat steps 3 a. through i. until all tissue samples are prepared.
5. While steps 3 and 4 are being completed someone needs to go to the NSRL irradiation facililty and prepare the area for the run. Check and clean surfaces, check incubators, and set up rocking platforms in incubator(s), As well as transport sample holders and fixative (cold MeOH:acetone (on ice)).
6. Warm bottles of distilled water to 37C.
7. Transport perfusion chambers in trays to NSRL irradiation facility
8. Replace medium, if lost in transit.
9. Hold perfusion chambers in incubator on rocking platform until irradiation.
10. Irradiate two samples at a time, in axial or transverse orientation. Perform sham irradiations mixed in with irradiations. Record time, dose and orientation to the beam.
11. Fix some samples immediately after irradiation with cold MeOH:Acetone for at least twenty minutes after rinsing with cold PBS in the chamber. Switch to 70% Ethanol thereafter.
12. Transfer the remainder of the samples to Medical division to hold in incubator.
13. Replace medium, if lost in transit.
14. Fix replicate samples at 4, 8 and 12 hour intervals with cold MeOH:acetone as above.
15. Trim and transfer samples to histology cassettes for transport to TAMU.
16. Ship samples and supplies to TAMU overnight.

APPENDIX B

CHAMBER HOLDER FOR HZE IRRADIATIONS

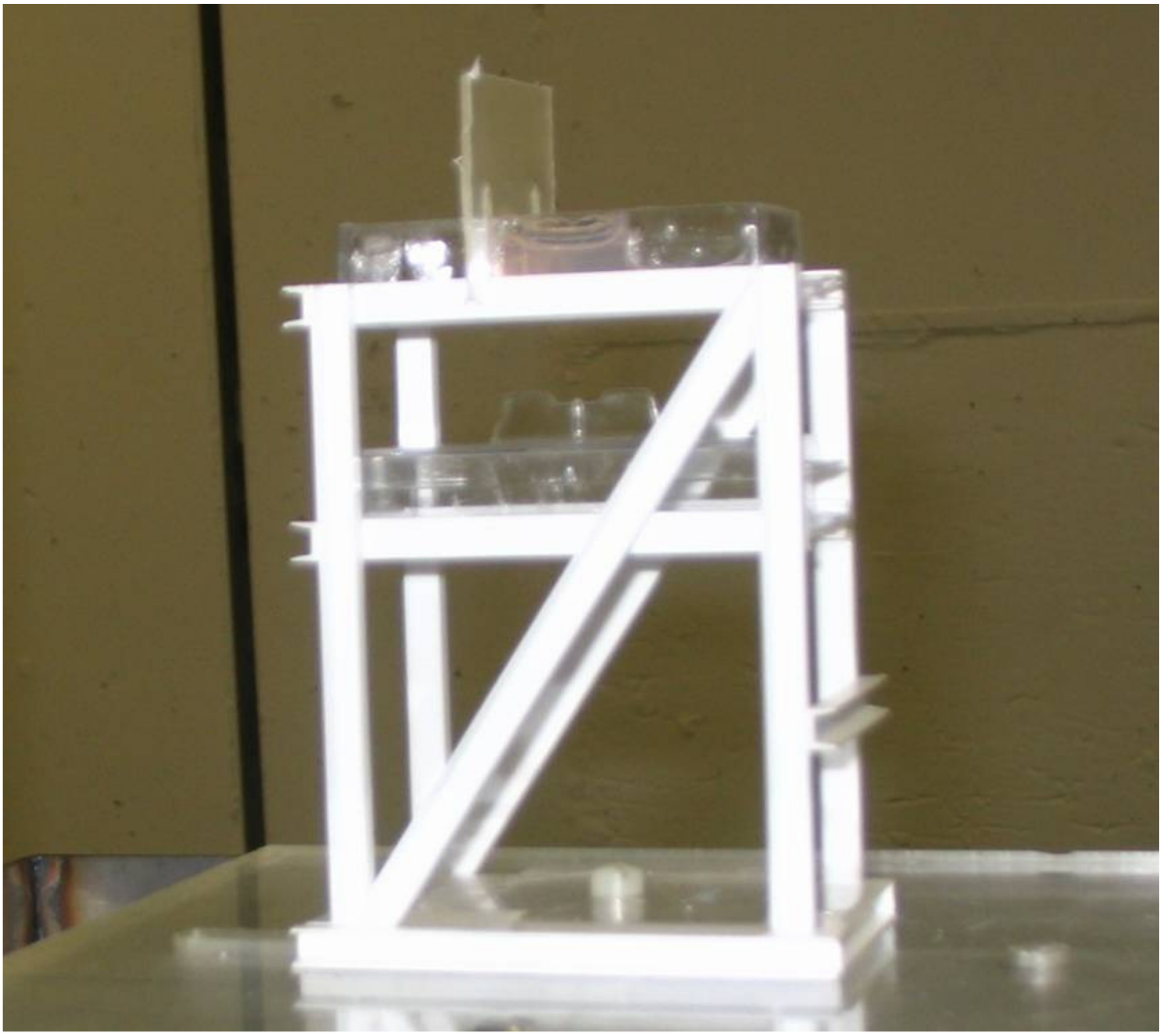

FIG. A-1. The irradiation holder for all tracheas irradiated at Brookhaven National Laboratory's HZE irradiation facility.

APPENDIX C

DATA SPREADSHEET

An electronic copy of the raw data used to generate the data and figures in this dissertation is available at the Thesis Office of Texas A&M University and at the following web address: https://lowdosedata.tamu.edu. The files include a list of all trachea samples, the original fluorescent images, the total fluorescence yield, the fluorescent yield for bins 25-75, error analysis information, and the figures seen above.

VITA

Name: Amy Jesse Maslowski

Address: Department of Nuclear Engineering, Texas A&M University, MS 3133, College Station, TX 77843-3133

Email Address: amymas@tamu.edu

Education: B.S., Physics, College of Charleston, 1999
Ph.D., Nuclear Engineering, Texas A&M University, August 2007.

Presentations: A. J. Maslowski, J. R. Ford, and L. A. Braby (Radiation Research Society, Denver, Colorado, 2005) Low Dose Radiation Interactions with the TGF-beta Pathway through ECM Components.

A. J. Maslowski, R. A. Redd, J. R. Ford, and L. A. Braby (Radiation Research Society Meeting, St. Louis, Missouri, 2004) Radiation Response of Tracheal Epithelium in Perfused Cultures.

J. R. Ford, A. J. Maslowski, and L. A. Braby (International Congress of Radiation Research, Brisbane, Australia, 2003) Radiation Response of Perfused Tracheal Sections.

Publications: J. R. Ford, A. J. Maslowski, R. A. Redd and L. A. Braby, Radiation Response of Perfused Tracheal Tissue, *Radiat. Res*. **164**, 487-492 (2005).

A. Adams, J. L. F. Bastos, H. J. Boado Magan, A. J. Houck (Maslowski), S. Kleitsas, S. Paranjpe and M. H. Voth. Analysis of Response to the IAEA Assessment Survey of Research Reactor Safety, http://www.iaea.org/ns/nusafe/publish/papers/asmtsrvy03.pdf, Jan. 2003.

A. J. Houck (Maslowski) and D. Timmons. The Chornobyl Accident: A Comprehensive Risk Assessment, *Health Phys*. **79(6):** 309 (2000).